Preprints (www.preprints.org) | NOT PEER-REVIEWED | Posted: 14 May 2018 doi:10.20944/preprints201805.0196.v1

Peer-reviewed version available at Molecules 2018, 23, 1401; doi:10.3390/molecules23061401

New tetrahydroisoquinoline derivatives overcome Pgp activity in brain-blood barrier and glioblastoma multiforme

Iris C. Salaroglio[1], Elena Gazzano[1], Joanna Kopecka[1], Konstantin Chegaev[2], Costanzo Costamagna[1], Roberta Fruttero[2], Stefano Guglielmo[2,*] and Chiara Riganti[1,*]

[1] Department of Oncology, University of Torino, via Santena 5/bis, 10126, Torino Italy

[2] Department of Drug Science and Technology, University of Torino, via Pietro Giuria 9, 10125, Torino, Italy

*Equal contribution

Corresponding authors: Dr. Stefano Guglielmo, Department of Drug Science and Technology, University of Torino, via Pietro Giuria 9, 10125, Torino, Italy; Phone: +390116707178; email: stefano.guglielmo@unito.it; Dr. Chiara Riganti, Department of Oncology, University of Torino, via Santena 5/bis, 10126, Torino Italy. Phone: +390116705857; email: chiara.riganti@unito.it

Abstract

P-glycoprotein (Pgp) determines resistance to a broad spectrum of drugs in glioblastoma multiforme (GB) because it is highly expressed in GB stem cells and in brain-blood barrier (BBB), the peculiar endothelium surrounding brain. Inhibiting Pgp activity in BBB and GB is still an open challenge. Here, we tested the efficacy of a small library of tetrahydroisoquinoline derivatives with an EC_{50} for Pgp $\leq$ 50 nM, in primary human BBB cells and in patients-derived GB, from which we isolated differentiated/adherent cells (AC, i.e. Pgp-negative/doxorubicin-sensitive cells) and stem cells (neurospheres, NS, i.e. Pgp-positive/doxorubicin-resistant cells). At 1 nM, 3 compounds increased the delivery of doxorubicin, a typical substrate of Pgp, across BBB monolayer, without altering expression and activity of other transporters. The compounds increased the drug accumulation

within NS, restoring necrosis, apoptosis and reduction in cell viability induced by doxorubicin. In co-culture systems, the compounds added to the luminal face of BBB increased the delivery of doxorubicin to NS growing under BBB and rescued the drug's cytotoxicity. Our work identified new ligands of Pgp active at low nanomolar concentrations, that effectively reduce Pgp activity in BBB and GB, and can improve chemotherapy efficacy in this tumor.

Keywords: P-glycoprotein; glioblastoma multiforme; brain-blood barrier; doxorubicin

Preprints (www.preprints.org) | NOT PEER-REVIEWED | Posted: 14 May 2018 doi:10.20944/preprints201805.0196.v1

Peer-reviewed version available at Molecules 2018, 23, 1401; doi:10.3390/molecules23061401

Introduction

Glioblastoma multiforme (GB) is considered the most common, aggressive and lethal brain tumor in adult population, because of the high infiltration into surrounding brain tissue. GB usually occurs within the white matter as a heterogeneous lesion, but it spreads rapidly into the surrounding brain tissue [1]. GB standard therapy involves surgical resection, followed by radiotherapy and chemotherapy based on temozolomide, followed by second-line therapy based on topoisomerase I and II inhibitors, or anti-angiogenic drugs. The success of chemotherapy is limited by the tumor polyclonality, the intrinsic resistance to most chemotherapeutic drugs and the presence of blood-brain barrier (BBB) [2-4].

Chemotherapy is not efficient to completely eradicate tumor stem cells (SCs) that contribute to initiation, progression and recurrence of GB. Indeed, these cells show a multidrug resistance (MDR) phenotype [5-6] that prevents the intracellular accumulation and efficacy of several antineoplastic drugs. The MDR phenotype of GB SCs is sustained by the high expression of ATP binding cassette (ABC) transporters, such as P-glycoprotein (Pgp/ABCB1), MDR related protein 1 (MRP1/ABCC1), breast cancer resistance protein (BCRP/ABCG2) [6].

Chemotherapy fails against GB also because of the low drug delivery across the BBB, the microvascular endothelium that surrounds brain parenchyma. BBB is characterized by the absence of fenestrations and the presence of tight junctions (TJs) and ABC transporters [7-8]. BBB is often disrupted within GB bulk, but it is competent in the “brain-adjacent to tumor” (BAT) area, where isolated GB cells can grow, inducing local tumor recurrence or spreading in other areas if not eradicated by chemotherapy [7]. Pgp is abundant on GB SCs and on the luminal side of BBB, and mediates the backward efflux of doxorubicin, taxanes, Vinca alkaloids, teniposide/etoposide, topotecan, methotrexate, imatinib, dasatinib, lapatinib, gefitinib, sorafenib, erlotinib [8].

Preprints (www.preprints.org) | NOT PEER-REVIEWED | Posted: 14 May 2018 doi:10.20944/preprints201805.0196.v1

Peer-reviewed version available at Molecules 2018, 23, 1401; doi:10.3390/molecules23061401

The presence of Pgp either in GB and BBB represents a double obstacle for the success of chemotherapy. Notwithstanding different approaches to circumvent the Pgp efflux activity in BBB [9-14] and GB, in particular in GB SCs [15-17], no satisfactory tools have been found.

Our research group has recently developed a library of Pgp ligands, based on the tetrahydroisoquinoline scaffold, a substructure often found in Pgp ligands [18-19]. The compounds were designed by functionalizing the phenolic group of an already known Pgp inhibitor [MC70, 20] with two types of substituents: 1,2,5-oxadiazole (furazan) moiety linked through alkyl spacers [18], and flexible alkyl chains of various length [19]. From this library, we selected 6 compounds with an EC_{50} for Pgp ranging from 0.60 nM to 54 nM (**Table 1**), i.e. superimposable with the last-generation of Pgp inhibitors [21].

Table 1. Structures and EC_{50} of Pgp ligands tested

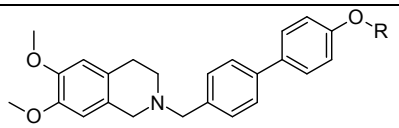

Compound	R	EC_{50} (nM)
1	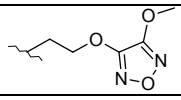	0.60[18]
2	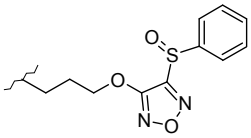	1.3[18]
3	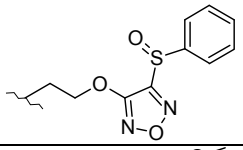	0.90[18]
4	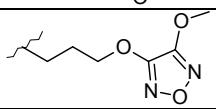	54[18]
5	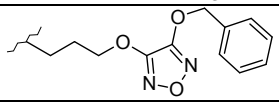	0.97[18]
6	*n*-(C_4H_9)-	5.2[19]
7 (MC70)	-H	690[20]

In the present work we investigated whether these compounds overcame the Pgp activity at BBB and GB levels. We used human brain microvascular endothelial cells and GB cells obtained from patients, isolated and propagated as differentiated (adherent cell, AC) or stem cell-enriched

Preprints (www.preprints.org) | NOT PEER-REVIEWED | Posted: 14 May 2018 doi:10.20944/preprints201805.0196.v1

Peer-reviewed version available at Molecules 2018, 23, 1401; doi:10.3390/molecules23061401

(neurospheres, NS) cultures. In isolated BBB and GB, as well as in co-culture systems, we studied the effects of Pgp ligands on the transport and accumulation on doxorubicin, chosen as a prototypical drug that does not cross BBB [12, 22] and is ineffective against GB NS [16], being a substrate of Pgp.

Results

Chemistry

Target compounds **1-5** [18] and **6** [19] were prepared as reported, starting from MC70. The latter one was more conveniently prepared according to a straightforward metal-free synthetic route depicted in **Scheme 1**.

Scheme 1. Synthesis of MC70.

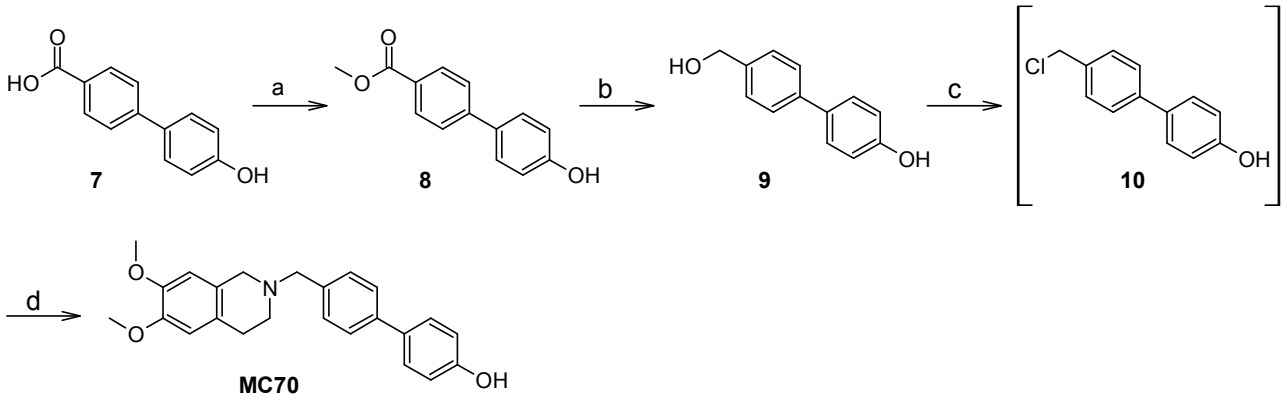

Reagents and conditions. a) CH_3OH, cat. conc. H_2SO_4, reflux, 90 min.; b) $LiAlH_4$, tetrahydrofuran, room temperature 45 min.; c) HCl 37%, 90 °C, 2 hours; d) 6,7-dimethoxy-1,2,3,4-tetrahydroisoquinoline hydrochloride, 4-methylmorpholine, CH_3CN, reflux, 6 hours.

Briefly, the commercially available 4'-hydroxybiphenyl-4-carboxylic acid **7** was converted into the corresponding methyl ester by refluxing in methanol with a catalytic amount of concentrated sulfuric acid. The product was reduced to the benzyl alcohol **9** in presence of $LiAlH_4$ at room temperature. Treatment of **9** with 37% HCl at 90 °C afforded the benzyl chloride **10** which was readily reacted with 6,7-dimethoxy-1,2,3,4-tetrahydroisoquinoline hydrochloride to give MC70.

Pgp ligands increase the delivery of doxorubicin across BBB monolayer

Preprints (www.preprints.org) | NOT PEER-REVIEWED | Posted: 14 May 2018 doi:10.20944/preprints201805.0196.v1

Peer-reviewed version available at Molecules 2018, 23, 1401; doi:10.3390/molecules23061401

In preliminary dose-dependent experiments, we verified the lack of toxicity of the compounds on human brain microvascular endothelial hCMEC/D3 cells monolayer. We detected a significant reduction in BBB cell viability only after 24 h of incubation with compounds **1-3** at 100 and 1000 nM. None of the compounds decreased cell viability at 1 nM (**Figure 1A**), a concentration around their EC_{50} on Pgp [18, 19] that was chosen for the following experiments. At this concentration the compounds did not change the expression of the ABC transporters Pgp, MRP1 and BCRP nor of TJ proteins claudin 3, claudin 5, occludin and zonula occludens-1 (ZO-1; **Figure 1B**). Compounds **1-3** - but not compounds **4-6** - significantly increased the delivery of doxorubicin, a virtually BBB-impermeable drug [12, 22], through hCMEC/D3 cells monolayer (**Figure 1C**). The permeability of mitoxantrone, an index of BCRP activity [12], was not affected (**Supplementary Figure 1**). Doxorubicin is also a substrate of MRP1 and BCRP; indeed, doxorubicin delivery across hCMEC/D3 cells monolayer was increased by the MRP1 inhibitor MK571 or by the BCRP inhibitor fumitremorgin C (**Supplementary Figure 2**). The effects of compounds **1-6,** however, was unaffected by MRP1 and BCRP inhibitors (**Supplementary Figure 2**). This may sound surprising since MK571 and fumitremorgin C alone increased the permeability of doxorubicin across hCMEC/D3 cells monolayer (**Supplementary Figure 2).** To clarify this issue, we tested the permeability of doxorubicin in MDCK cells selectively overexpressing Pgp, MRP1 or BCRP (**Supplementary Figure 3A**), treated with compounds **1-6**. As shown in the new **Supplementary Figure 3B-D** compounds **1-3** increased doxorubicin permeability across Pgp-MDCK monolayer, but reduced the drug transport across MRP1-MDCK or BCRP-MDCK monolayer. This result can suggest an activation of drug efflux activity by MRP1 and BCRP, explaining the lack of increase of doxorubicin transport induced by compounds **1-3** in the presence of MRP1 or BCRP inhibitors. As expected, the Pgp inhibitor verapamil increased doxorubicin permeability in untreated Pgp-MDCK cells and in cells treated with the Pgp ligands: the extent of such increase was higher in cells exposed to compounds **1**, **2** and **3**, and similar to the control sample in cells treated with compounds **4**, **5** and **6** (**Supplementary Figure 3B**). Surprisingly, compounds **1**, **2** and **3** slightly reduced

Preprints (www.preprints.org) | NOT PEER-REVIEWED | Posted: 14 May 2018 doi:10.20944/preprints201805.0196.v1

Peer-reviewed version available at *Molecules* **2018**, *23*, 1401; doi:10.3390/molecules23061401

doxorubicin delivery in MRP1-MDCK (**Supplementary Figure 3B**) and in BCRP-MDCK (**Supplementary Figure 3D**) cells. Moreover, compounds **4**, **5** and **6**, which did not change doxorubicin transport in Pgp-MDCK cells, except in the presence of verapamil, strongly reduced doxorubicin transport in MRP1-MDCK and BCRP-MDCK cells. These effects were reversed by MK571 and fumitremorgin C, respectively (**Supplementary Figures 3B-D)**.

Preprints (www.preprints.org) | NOT PEER-REVIEWED | Posted: 14 May 2018 doi:10.20944/preprints201805.0196.v1

Peer-reviewed version available at Molecules 2018, 23, 1401; doi:10.3390/molecules23061401

Figure 1

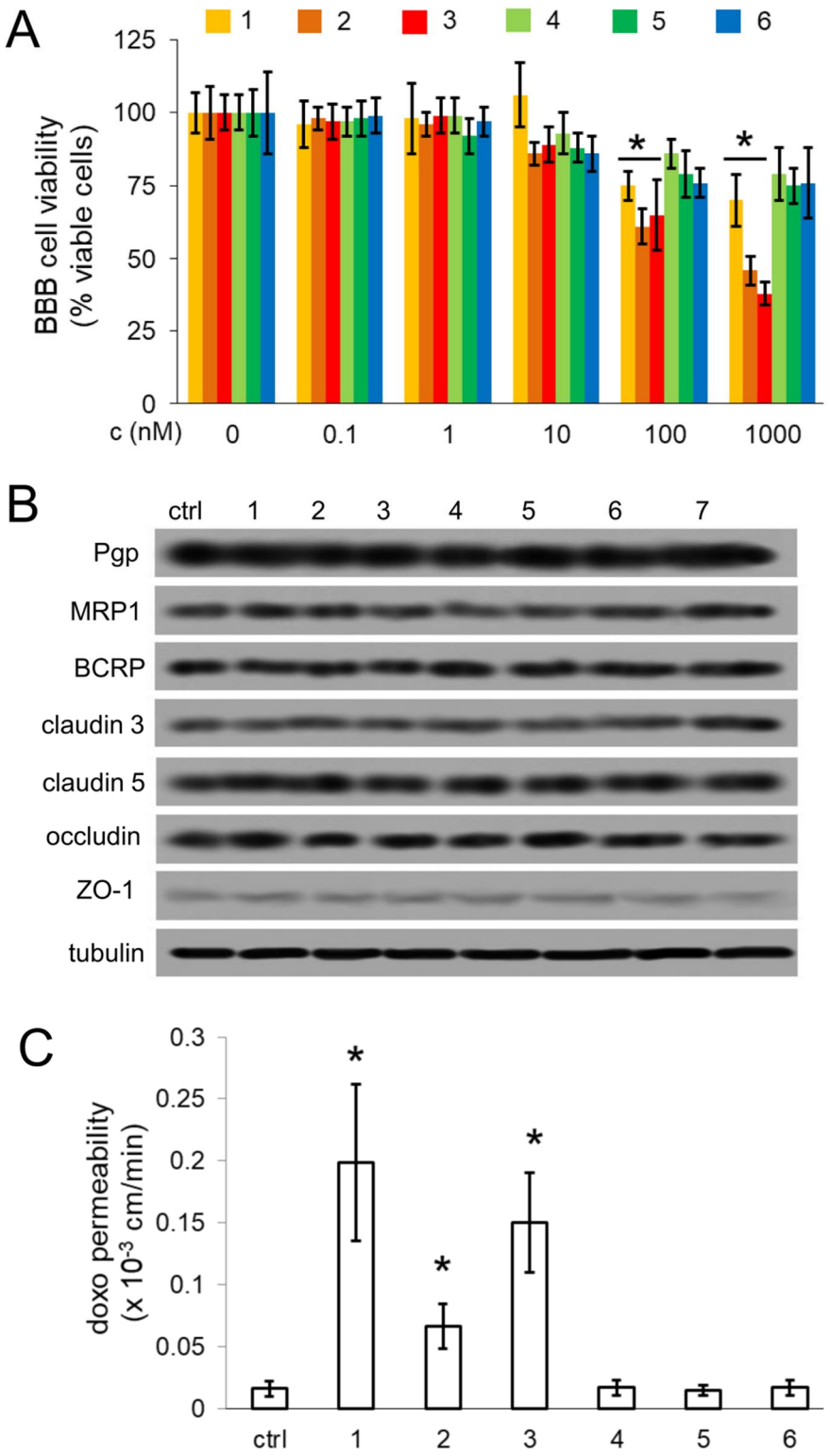

The transendothelial electrical resistance TEER value of BBB monolayer was between 28 and 38 Ω cm^2, the permeability coefficient of 70-kDa dextran-fluorescein-isothiocyanate (FITC), an index of TJs integrity [23] was $0.21 \pm 0.05 \times 10^{-3}$ cm min^{-1}, the permeability coefficients of [^{14}C]-sucrose,

Preprints (www.preprints.org) | NOT PEER-REVIEWED | Posted: 14 May 2018 doi:10.20944/preprints201805.0196.v1

Peer-reviewed version available at Molecules 2018, 23, 1401; doi:10.3390/molecules23061401

[^{14}C]-inulin and lucifer yellow, indexes of paracellular diffusion [22-24] were $1.28 \pm 0.19 \times 10^{-3}$ cm min^{-1}, $0.45 \pm 0.07 \times 10^{-3}$ cm min^{-1} and $0.43 \pm 0.11 \times 10^{-3}$ cm min^{-1}. These values were in line with previous findings [12, 22-24], suggesting the functional integrity of the BBB monolayer. None of the compounds changed the TEER of BBB monolayer a 1 nM, while at 100 nM compounds **1-3** decreased TEER values indicating the loss of BBB integrity at these concentrations (**Table 2**). None of the compounds changed the permeability of 70-kDa dextran, [^{14}C]-inulin, [^{14}C]-sucrose and lucifer yellow (**Supplementary Figure 4A-D**).

Table 2. TEER values of BBB monolayer treated with Pgp ligands

Compound	TEER (Ω cm^2) compound 1 nM	TEER (Ω cm^2) compound 100 nM
ctrl	31 ± 2	30 ± 3
1	33 ± 3	41 ± 2 *
2	29 ± 1	39 ± 2 *
3	35 ± 3	44 ± 4 *
4	34 ± 4	33 ± 3
5	36 ±3	34 ±5
6	33 ± 2	31 ± 4

hCMEC/D3 cells were grown in the upper insert of Transwell devices for 7 days. The medium was then replaced with fresh medium (ctrl) or with medium containing 1 nM or 100 nM of compounds **1-6** for 24 h. TEER was measured in duplicates. 100 nM vs 1 nM: * $p < 0.05$. Data are presented as means ± SD (n = 4). TEER values are subtracted from the mean TEER value obtained in the absence of cells.

Pgp ligands increase doxorubicin uptake and cytotoxicity in Pgp-positive neurosphere from glioblastoma

We next validated the efficacy of our compounds against primary GB cells of 3 patients. From each tumor, AC and NS were generated (**Figure 2A**). As previously shown [16], NS had typical stemness properties, such as self-renewal, *in vitro* clonogenicity and *in vivo* tumorigenicity. In parallel, NS had high expression of general and neural stemness markers (nestin, CD133, Musashi, SOX2, EGFR, p53) and low expression of differentiation markers (glial fibrillary acidic protein, GFAP; galactocerebroside-C, Gal-C) compared to AC (**Supplementary Table 1**), suggesting that they represent cultures enriched in GB-derived SCs. As shown in **Figure 2B**, AC had undetectable

Preprints (www.preprints.org) | NOT PEER-REVIEWED | Posted: 14 May 2018 doi:10.20944/preprints201805.0196.v1

Peer-reviewed version available at *Molecules* **2018**, *23*, 1401; doi:10.3390/molecules23061401

levels of Pgp and low levels of MRP1 and BCRP; by contrast, all these ABC transporters were well-detected in the corresponding NS. In keeping with this trend, fluorescence microscope analysis revealed a typical intranuclear localization of doxorubicin in AC, whereas NS had no appreciable red fluorescence, indicating a very low drug uptake (**Figure 2C**). This difference was confirmed by the quantitative fluorimetric measurement of doxorubicin uptake in AC and NS (**Figure 2D**). NS, which had a lower intracellular retention of the drug compared to AC, significantly increased doxorubicin accumulation if treated with compounds **1-3**. Compounds **4-6** had no effects. Moreover, none of the compounds increased the drug uptake in AC compared to untreated cells (**Figure 2D**).

Preprints (www.preprints.org) | NOT PEER-REVIEWED | Posted: 14 May 2018 doi:10.20944/preprints201805.0196.v1

Peer-reviewed version available at Molecules 2018, 23, 1401; doi:10.3390/molecules23061401

Figure 2

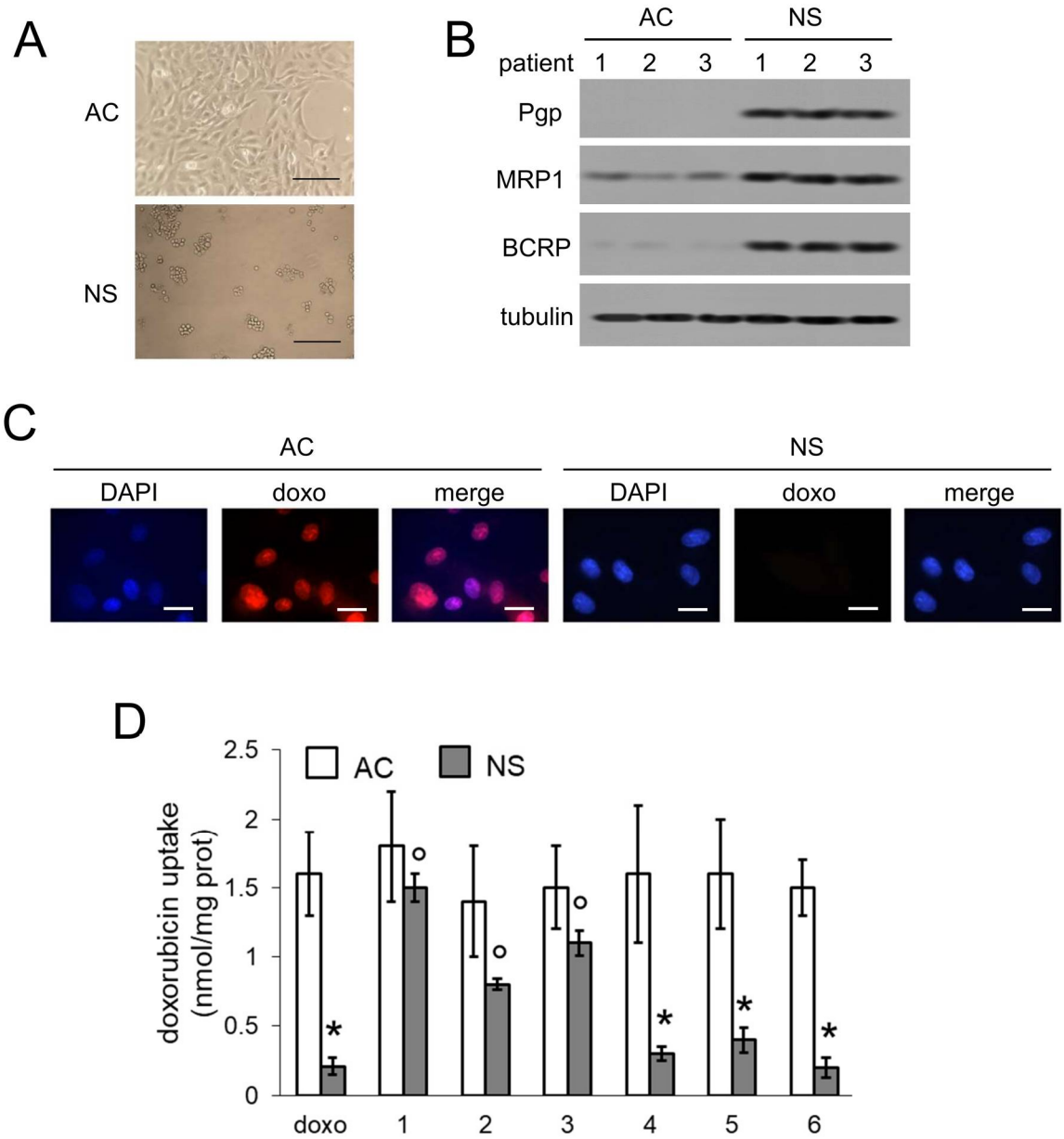

Pgp ligands were not toxic on GB cells: indeed, they did not increase the release of lactate dehydrogenase (LDH; **Figure 3A**), indicative of cell damage and necrosis [16], they did not activate caspase 3 (**Figure 3B**), an index of apoptosis, and they did not reduce AC and NS viability (**Figure 3C**). According to the higher retention of doxorubicin in AC than in NS, the drug increased LDH release and caspase 3 activity, and decreased cell viability in AC but not NS. Compounds **1-3** partially restored doxorubicin's cytotoxic effects in NS. Again the compounds did not enhance the

Preprints (www.preprints.org) | NOT PEER-REVIEWED | Posted: 14 May 2018 doi:10.20944/preprints201805.0196.v1

Peer-reviewed version available at Molecules 2018, 23, 1401; doi:10.3390/molecules23061401

anthracycline's effects in AC. Compounds **4-6** – that did not increase doxorubicin accumulation in NS (Figure **2D**) – were unable to restore the drug's toxicity as well (**Figure 3A-C**).

Figure 3

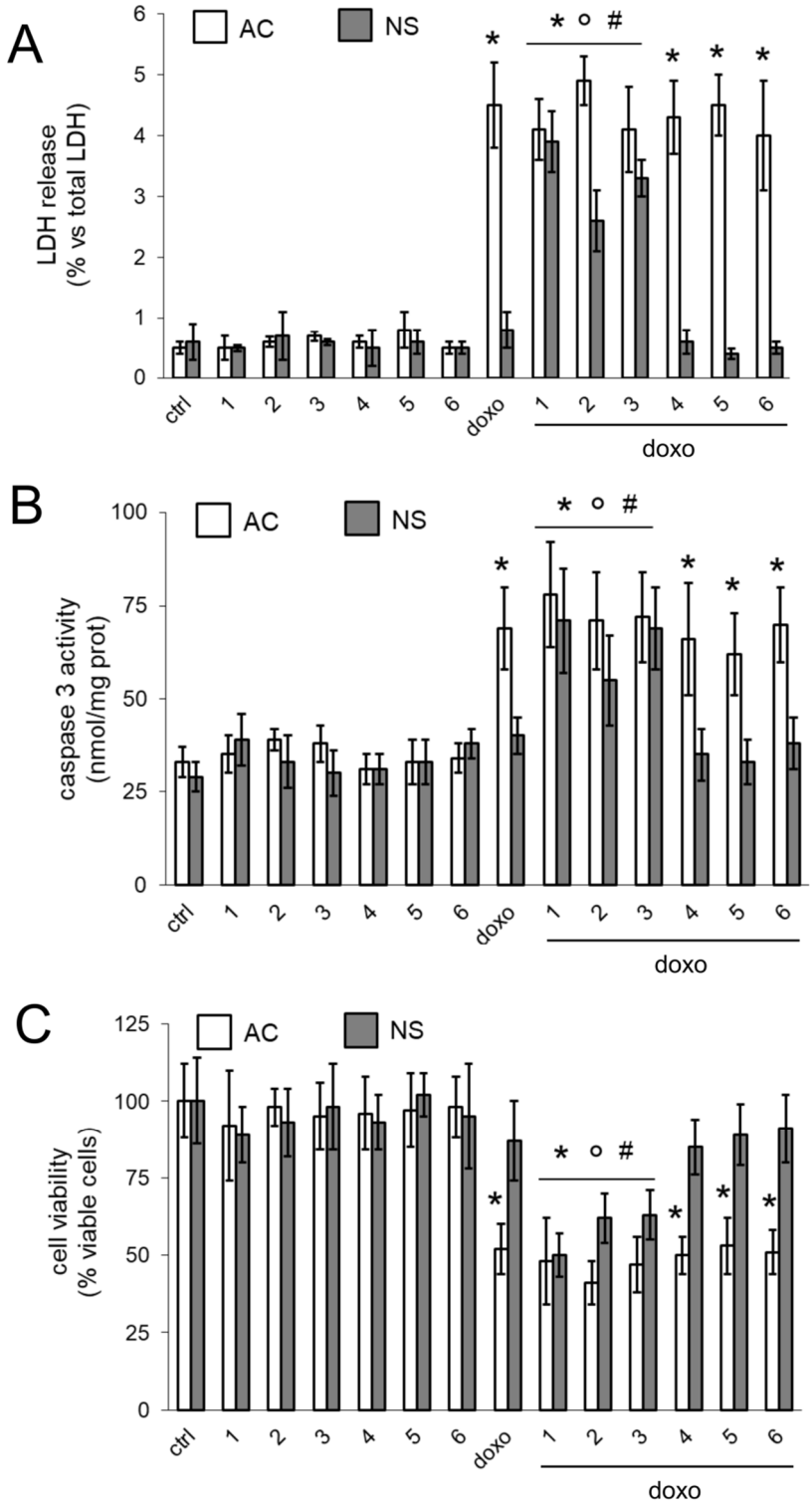

Pgp ligands increase the intra-tumor delivery and cytotoxicity of doxorubicin in BBB-glioblastoma co-cultures

Preprints (www.preprints.org) | NOT PEER-REVIEWED | Posted: 14 May 2018 doi:10.20944/preprints201805.0196.v1

Peer-reviewed version available at Molecules 2018, 23, 1401; doi:10.3390/molecules23061401

We finally validated the efficacy of our Pgp ligands in co-culture systems: doxorubicin-resistant NS were seeded in the lower chamber of Transwell devices, containing confluent hCMEC/D3 monolayer in the upper chamber. Doxorubicin, alone or co-incubated with compounds, was added in the upper chamber, facing the luminal side of BBB cells. In these conditions, the amount of doxorubicin delivered into NS (**Figure 4A**) was unable to elicit cell necrosis (**Figure 4B**) and apoptosis (**Figure 4C**), nor to decrease NS viability (**Figure 4D**). The co-incubation with compounds **1-3** significantly increased the amount of doxorubicin delivered to NS (**Figure 4A**), the release of LDH (**Figure 4B**) and the activity of caspase 3 (**Figure 4C**). At longer time-point NS viability was also reduced by the co-incubation of doxorubicin and compounds **1-3** (**Figure 4D**).

Figure 4

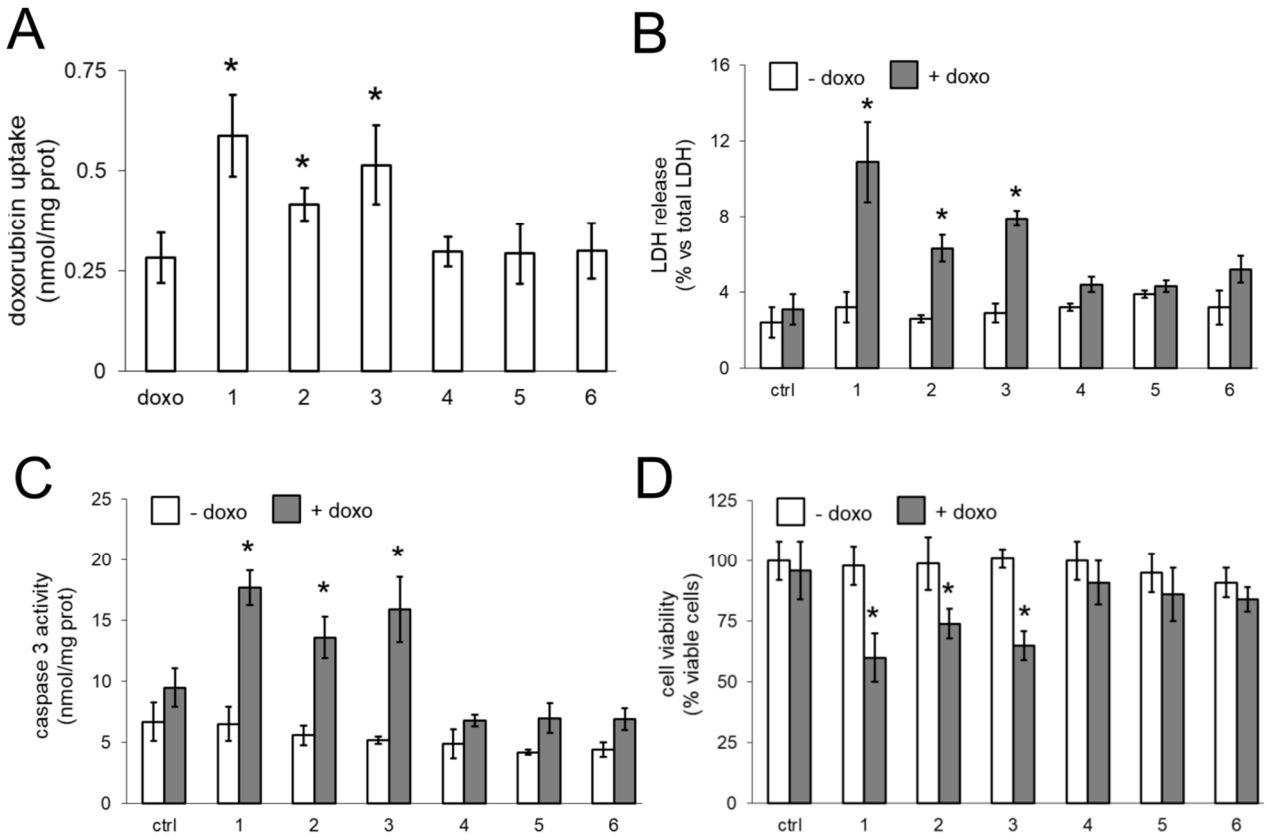

To discriminate whether the effects of the Pgp ligands were solely due to the inhibition of Pgp on BBB, or to their inhibitory effects on Pgp both on BBB and NS (i.e. after crossing the barrier), we added 5 µM doxorubicin, alone or with compound **1-6**, in the upper chamber of Transwell devices

Preprints (www.preprints.org) | NOT PEER-REVIEWED | Posted: 14 May 2018 doi:10.20944/preprints201805.0196.v1

Peer-reviewed version available at Molecules 2018, 23, 1401; doi:10.3390/molecules23061401

containing BBB. After 3 h, the medium of the lower chamber was collected: part was added to on NS cultures (Figure 5**A**), part was used to measure the doxorubicin concentration (Figure 5**B**). The drug concentration in the media of the lower chamber ranged between 1 and 1.8 μM for the Transwells treated with compounds **1-3**, and was significantly higher than in all the other experimental conditions (Figure 5**B**). The effects elicited by the media derived from these Transwells was compared with the effects produced by medium containing 1 μM doxorubicin. Of note, the intracellular doxorubicin uptake in NS (Figure 5**C**), the release of LDH (Figure 5**D**), the activity of caspase-3 (Figure 5**E**) were higher, the viability of NS was lower (Figure 5**F**) when NS were treated with media derived from Trasnwells exposed to compounds **1-3** than with medium containing 1 μM doxorubicin, suggesting a possible effects of the compounds on Pgp either in BBB cells or in NS.

Preprints (www.preprints.org) | NOT PEER-REVIEWED | Posted: 14 May 2018 doi:10.20944/preprints201805.0196.v1

Peer-reviewed version available at *Molecules* **2018**, *23*, 1401; doi:10.3390/molecules23061401

Figure 5

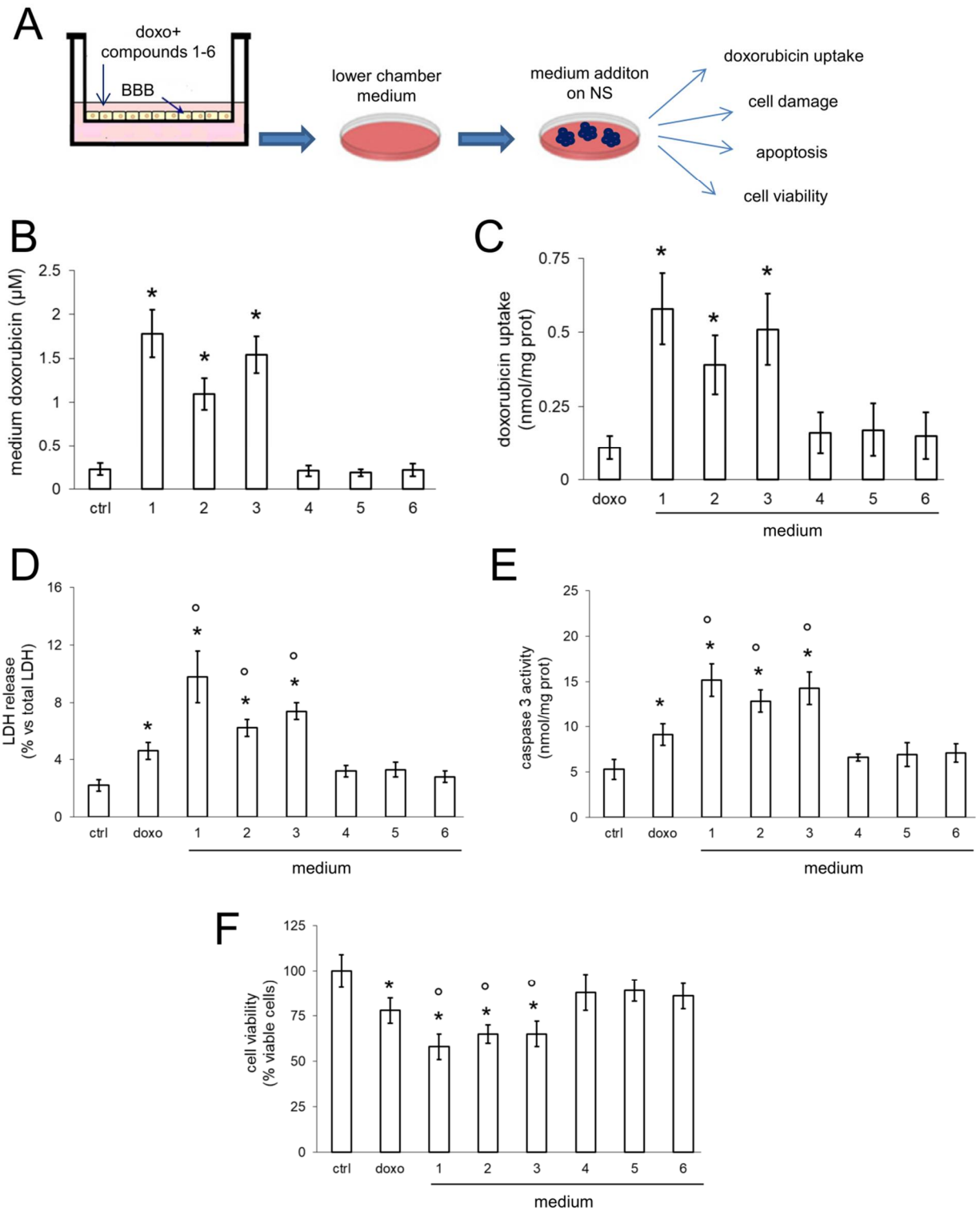

Discussion

Preprints (www.preprints.org) | NOT PEER-REVIEWED | Posted: 14 May 2018 doi:10.20944/preprints201805.0196.v1

Peer-reviewed version available at Molecules 2018, 23, 1401; doi:10.3390/molecules23061401

Many Pgp inhibitors that achieved excellent efficacy *in vitro* had failed in pre-clinical and clinical models because of the great toxicity, owing to the high concentrations (i.e. millimolar-micromolar concentrations) needed to inhibit Pgp, that induced heavy side-effects and toxicities [25]. Looking for more effective P-glycoprotein inhibitors, it was observed that Pgp-expressing tumor cells retain sensitivity to local anaesthetics, detergents, antimetabolites, alkylating agents, platinum compounds, metal chelators. These findings opened the opportunity to bypass MDR by treating Pgp-expressing cells with non-cross-resistant drugs, exploiting the peculiar sensitivity of resistant cells to these agents (i.e., exploiting the so-called "collateral sensitivity", CS) [26]. Despite promising results *in vitro*, the *in vivo* safety of these agents, most of which exert cytotoxic effects in cell cultures, is not known.

Targeting ABC efflux transporters with new chemosensitizers is still considered the main strategy to improve drug delivery and overcome MDR [27], but it remains an unmet need. Compared to the first Pgp inhibitors, the latest generation of Pgp inhibitors, such as tariquidar, elacridar or zosuquidar, showed efficacy at lower concentrations (i.e. nanomolar concentrations) and higher specificity for Pgp over the other ABC transporters [21].

Furazan based compounds **1-5** were originally designed following some preliminary results on the activity of some furazan derivatives towards Pgp (unpublished data): in this series, stereo-electronic properties of the substituents on the heterocyclic ring were modulated. Compound **6** belongs to a series of derivatives designed mainly with the aim of verifying the effect of lipophilicity of the substituents on the phenolic group of parent compound. As can be seen from EC_{50} values, the selected MC70 derivatives proved much more potent and displayed a functional profile different compared to MC70: the latter behaves as a Pgp inhibitor, since it has an apparent permeability ratio < 2, determined in Caco-2 cells monolayer, and does not induce ATP depletion; the new compounds are substrates belonging to a particular class defined as class IIB3, characterized by apparent permeability > 2 and absence of ATP depletion [18, 19]. Kinetic parameters for these derivatives have not been determined, but, as a cautious consideration, it can be argued that, due to

Preprints (www.preprints.org) | NOT PEER-REVIEWED | Posted: 14 May 2018 doi:10.20944/preprints201805.0196.v1

Peer-reviewed version available at Molecules 2018, 23, 1401; doi:10.3390/molecules23061401

the large internal cavity of Pgp, binding of ligands could be approximately considered only diffusion-limited; in such cases, a typical residence time for nanomolar ligands would be around 1 s [28].

3 out of 6 compounds, namely **1-3**, effectively increased the transport of doxorubicin, a virtually BBB-impermeable drug, being a substrate of Pgp [7], across BBB monolayer, when used at 1 nM concentration. Notably, at such concentration they did not reduce BBB cell viability and they did not change expression of other luminal ABC transporters and TJ proteins, nor they modify TEER values. This experimental set demonstrated that at this concentration the compounds do not compromise the integrity and the physiological properties of BBB. Of note, compounds **1-3** strongly inhibited Pgp activity, but slightly activated MRP1 and BCRP, as demonstrated by the increased transport of doxorubicin across Pgp-MDCK monolayer, the decreased transport across MRP1-MDCK and BCRP-MDCK monolayer, by the lack of increase in doxorubicin transport across hCMEC/D3 monolayer treated with MRP1 and BCRP inhibitors compared to untreated cells. These contrasting effects may reduce the efficacy of compounds **1-3** on doxorubicin transport: on the one hand the compounds increased the drug delivery by inhibiting Pgp, on the other hand they decreased the drug transport by stimulating MRP1 and BCRP. The activating effect on MRP1 and BCRP, however, was smaller compared to the inhibitory effect on Pgp, in terms of doxorubicin transport, as demonstrated by the results in MDCK cells selectively expressing Pgp, MRP1 or BCRP: therein, the net effect in hCMEC/D3 cells, where these three transporters were present, was a significant increase of the transport of doxorubicin across BBB monolayer. Compounds **4**, **5** and **6** did not affect doxorubicin transport across Pgp-MDCK cells, where MRP1 and BCRP levels were undetectable, but they strongly reduced the drug transport in MRP1 and BCRP-MDCK cells, where Pgp was undetectable. This results suggest that compounds **4**, **5** and **6** were likely activators of MRP1 and BCRP, but the activating effect was reversed by selective MRP1 and BCRP inhibitors According to the results obtained with compounds **1-3** (inhibitors of doxorubicin transport by Pgp, slight activators of doxorubicin transport by MRP1 and BCRP) and with compounds **4-6** (neither

Preprints (www.preprints.org) | NOT PEER-REVIEWED | Posted: 14 May 2018 doi:10.20944/preprints201805.0196.v1

Peer-reviewed version available at Molecules 2018, 23, 1401; doi:10.3390/molecules23061401

inhibitors nor activators of doxorubicin transport by Pgp, strong activators of doxorubicin transport by MRP1 and BCRP), we can hypothesize that in hCMEC/D3 cells the main transporter involved in doxorubicin transport is Pgp, while MRP1 and BCRP play an ancillary role. We hypothesize that this could be the reason why we did not detect any effect of compounds **4-6** on doxorubicin delivery across BBB monolayer. We are aware that all the compounds exerted an inhibition on Pgp activity, measured as calcein-acetoxy methylester (AM) transport (Table 1). Given the complex structure of Pgp, containing different drug binding sites and characterized by different affinity for different substrates, it is not surprising that compounds inhibiting the transport of one substrate, have no effect or even opposite effects on the transport of other substrates [29]. Since our aim was to obtain a net increase in doxorubicin delivery across BBB to make it an effective anti-GB drug, the most promising compounds in this perspective were **1**, **2** and **3**.

All the compounds did not change the permeability of high molecular weight (70-kDa dextran) or low molecular weight ([^{14}C]-inulin, [^{14}C]-sucrose, lucifer yellow) compounds. Therefore, we excluded that the effects on doxorubicin permeability was due to loss of TJs integrity of change in paracellular diffusion of the drug across BBB.

Overall, our compounds showed the same properties – i.e. efficacy at low nanomolar concentrations, specificity for Pgp and lack of *in vitro* toxicities on not-transformed cells – of the latest generation of Pgp inhibitors or tracers, under investigation in preclinical models and clinical trials [10, 14, 21].

The selectivity for Pgp was demonstrated also in the experiments performed on AC and NS generated from patients GB. While AC where low Pgp-expressing cells and retained high amount of doxorubicin, NS were chosen as a prototypical model of highly Pgp-expressing GB-derived SCs (16). We recognize that NS do not reproduce the tissue organization and cell polarity occurring *in vivo* in the microvascular niches, where endothelial cells, pericytes, astroglial and microglial cells, differentiated and GB SCs, actively proliferating and apoptotic/necrotic GB cells were present and interconnected. However, NS have been proven to be a reliable tool to measure the

Preprints (www.preprints.org) | NOT PEER-REVIEWED | Posted: 14 May 2018 doi:10.20944/preprints201805.0196.v1

Peer-reviewed version available at Molecules 2018, 23, 1401; doi:10.3390/molecules23061401

chemosensitizing efficacy of Pgp-reversing agents in GB and BBB-GB co-cultures (12, 13, 16). We thus compared the effects of our compounds on AC and NS, alone and growing under hCMEC/D3 monolayer. The compounds did not exert any additive effects to doxorubicin in AC, where Pgp was undetectable. In AC, doxorubicin likely reached its maximal accumulation and exerted a broadest spectrum of cytotoxic effects, including cell necrosis, apoptosis and reduced viability. By contrast, the presence of Pgp in NS limited the retention and cytotoxic efficacy of doxorubicin. In NS compounds **1-3** restored the drug's accumulation to the same levels of AC, suggesting that they were able to inhibit the drug efflux via Pgp. As already observed in BBB, the compounds alone were not toxic against GB cells. Only the association of compounds and doxorubicin induced cytotoxicity, suggesting that the compounds acted as chemosensitizers agents, rescuing the efficacy of doxorubicin.

We could not directly demonstrate the transport of compounds **1-3** across BBB, since nanomolar concentrations were below the detection limit of high-pressure liquid chromatography (HPLC) device and micromolar concentrations, that were well-measured by HPLC, reduced cell viability of BBB, leading to suppose that at this concentration BBB is damaged and does not represent a physiologically competent BBB. However, in co-culture experiments, when we exposed the luminal side of BBB with the association of compounds **1-3** and doxorubicin, we observed an increased delivery and cytotoxicity of doxorubicin in NS growing under competent BBB. In BBB monolayer, Pgp is expressed on the luminal side [30], i.e. facing doxorubicin. The increased efficacy of doxorubicin may be due to a simple increase in the drug delivery across BBB, consequent to the inhibition of Pgp present on BBB. However, also NS express Pgp. According to the low intracellular retention of doxorubicin within NS, it is likely that Pgp is expressed on the outer surface of the spheres, preventing the intracellular accumulation of the drug.

Therein, doxorubicin delivered across BBB could not be efficiently accumulated within NS and exert its cytotoxic effects if the Pgp present in NS was active. The results of the experiments with medium collected from the lower chamber of Transwell devices incubated with compounds **1-3**

Preprints (www.preprints.org) | NOT PEER-REVIEWED | Posted: 14 May 2018 doi:10.20944/preprints201805.0196.v1

Peer-reviewed version available at Molecules 2018, 23, 1401; doi:10.3390/molecules23061401

suggest that the compounds inhibit at the same time Pgp on BBB and NS cells: this could be an indirect evidence of the delivery of compounds **1-3** across BBB. We are currently testing this hypothesis evaluating the pharmacokinetic profile of the compounds systemically administered in mice bearing orthotopically implanted GB.

Notwithstanding the excellent anti-tumor activity against GB in *in vitro* [31], doxorubicin is not a first-choice drug in GB treatment because of the very low delivery across BBB. However, since GB AC are sensitive to doxorubicin [31], several strategies to improve the *in vivo* efficacy of doxorubicin are under intensive investigation in pre-clinical and clinical settings [32-34]. Our compounds represent a step forward this direction, since they transformed the BBB-impermeable doxorubicin into a drug with a good BBB permeability and efficacy against Pgp-positive NS.

Moreover, temozolomide, topoisomerase I and II inhibitors, that are the current first- and second-line therapy in GB, are substrates of Pgp [11, 35]. Therein, this work may open the way to pre-clinical studies combining our Pgp ligands and these drugs, in order to circumvent Pgp-mediated chemoresistance and improve the efficacy of chemotherapy against GB.

Materials and methods

Chemicals. The plasticware for cell cultures was obtained from Falcon (Becton Dickinson, Franklin Lakes, NJ). The electrophoresis reagents were obtained from Bio-Rad Laboratories (Hercules, CA). The protein content of cell lysates was assessed with the BCA kit from Sigma Chemicals Co. (St. Louis, MO). Unless specified otherwise, all reagents were purchased from Sigma Chemicals Co.

Synthesis and characterization of compounds. ^{1}H and ^{13}C-NMR spectra were recorded on a Jeol 600 at 600 and 150 MHz respectively, using $SiMe_4$ as the internal reference. Chemical shifts (δ) are given in parts per million (ppm). The following abbreviations are used to designate the multiplicities: s = singlet, d = doublet, dd = doublet of doublets, t = triplet, q = quartet, m = multiplet. Low resolution mass spectra were recorded on a Micromass Quattro microTM API

Preprints (www.preprints.org) | NOT PEER-REVIEWED | Posted: 14 May 2018 doi:10.20944/preprints201805.0196.v1

Peer-reviewed version available at Molecules 2018, 23, 1401; doi:10.3390/molecules23061401

(Waters Corporation, Milford, MA, USA) with electrospray ionization. Melting points (mp) were determined with a capillary apparatus (Büchi 540). Flash column chromatography was performed on silica gel (Merck Kieselgel 60, 230-400 mesh ASTM). The progress of the reactions was followed by thin layer chromatography (TLC) on 5×20 cm plates with a layer thickness of 0.2 mm. The purity of target compounds was assessed by RP-HPLC. Analyses were performed on a HP1100 chromatograph system (Agilent Technologies, Palo Alto, CA, USA). The analytical column was a LiChrosphere® C18 5µM (Merck KGaA, 64271 Darmstadt, Germany). UV signals were recorded at 210, 226 and 254 nm. All compounds were dissolved in eluent and injected through a 20 µL loop. Compounds **1-5** and **6** were synthesized as previously detailed [18, 19].

Methyl 4'-hydroxybiphenyl-4-carboxylate (8). 4'-hydroxybiphenyl-4-carboxylic acid **7** was dissolved in methanol; to the solution 5 µL of concentrated sulfuric acid were added and the mixture was refluxed for 90 minutes. A white solid separated from the boiling mixture which was isolated by filtration. Yield: 78%. Mp = 231.1 - 231.5 °C. MS ESI$^-$: 227 [M-1]$^-$. ^{1}H-NMR (DMSO-d_6) δ 9.79 (s. 1H, C_6H_4O*H*), 7.97 (d, *J* = 8.3 Hz, 2H), 7.72 (d, *J* = 8.6 Hz, 2H), 7.58 (d, *J* = 8.6 Hz, 2H), 6.88 (d, *J* = 8.6 Hz, 2H), 3.85 (s, 3H, OCH_3). ^{13}C-NMR (DMSO-d_6) δ 166.16, 158.08, 144.73, 129.79, 129.40, 128.20, 127.31, 125.97, 115.94, 52.06.

4'-(Hydroxymethyl)biphenyl-4-ol (9). $LiAlH_4$ (1.3 eq) was suspended in anhydrous tetrahydrofuran under N_2 atmosphere. A solution of **8** in anhydrous tetrahydrofuran was added through a dropping funnel and the mixture was stirred at room temperature for 45 minutes. The mixture was then cooled in an ice bath and was quenched with ice-cold water and 1M HCl. The aqueous phase was then extracted with ethyl acetate; the organic extracts were washed with brine, dried over Na_2SO_4, filtered and evaporated under reduced pressure to afford the title product as a white solid in 89% yield. Mp = 204.2 - 205.0 °C (dec.). MS ESI$^-$: 227 [M-1]$^-$. ^{1}H-NMR (DMSO-d_6) δ 9.54 (s. 1H, C_6H_4O*H*), 7.53 (d, J = 8.3 Hz, 2H), 7.47 (m, 2H), 7.35 (d, J = 8.3 Hz, 2H), 6.85 (m,

Preprints (www.preprints.org) | NOT PEER-REVIEWED | Posted: 14 May 2018 doi:10.20944/preprints201805.0196.v1

Peer-reviewed version available at Molecules 2018, 23, 1401; doi:10.3390/molecules23061401

2H), 5.2 (t, J = 5.7 Hz, 1H, CH_2O*H*), 4.52 (d, J = 5.9 Hz, 2H, C*H*$_2$OH). ^{13}C-NMR (DMSO-d_6) δ 157.02, 140.65, 138.68, 130.91, 127.64, 127.04, 125.68, 115.74 67.2.

[4'-(6,7-Dimethoxy-3,4-dihydro-1H-isoquinolin-2-ylmethyl)biphenyl-4-ol] (MC70). Compound **9** was suspended in 37% HCl and the mixture was stirred at 90 °C for 2 hours. The suspension was cooled in an ice bath, diluted with ice-cold water and filtered under reduced pressure to give **10** as a white solid, which, after being dried over KOH, was dissolved in acetonitrile. To the solution 6,7-dimethoxy-1,2,3,4-tetrahydroisoquinoline hydrochloride (1.3 eq) and 4-methylmorpholine (2.3 eq) were added and the mixture was refluxed for 6 hours. The solvent was then evaporated under reduced pressure, the residue was taken up with water and extracted with ethyl acetate. The organic extracts were washed with brine, dried over Na_2SO_4, filtered and evaporated under reduced pressure. The crude product was purified on silica gel column, eluting with petroleum ether / acetone 70 / 30, to give the title product identical to an authentic sample [19]. Yield 56% over two steps.

The Pgp activity in the presence of compounds was evaluated by the Calcein-AM assay and the bioluminescent ATP assay, as described previously [18, 19].

BBB cells, TEER and permeability assays. hCMEC/D3 cells, a human brain microvascular endothelial stabilized cell line, were a kind gift from Prof. Pierre-Olivier Couraud (Institut Cochin, Centre National de la Recherche Scientifique UMR 8104, INSERM U567, Paris, France) and were cultured according to [22]. Cells were seeded at 50,000/cm² density, and grown for 7 days up to confluence in 6-well Transwell devices (0.4 µm diameter pores-size, Transwell insert surface: 4.67 cm^2; Corning Life Sciences, Chorges, Francefor transport assays) or 24-well Transwell devices (0.4 µm diameter pores-size, Transwell insert surface: 0.33 cm^2; Corning Life Sciences for TEER measure), to allow the formation of a competent BBB. Before each experiment, TEER and permeability coefficients of 70 kDa-Dextran FITC, [^{14}C]-sucrose (589 mCi/mmol; PerkinElmer, Waltham, MA), [^{14}C]-inulin (10 mCi/mmol; PerkinElmer) and lucifer yellow (Invitrogen Life

Peer-reviewed version available at Molecules 2018, 23, 1401; doi:10.3390/molecules23061401

Technology, Milano, Italy), were measured as previously described [12, 22-24] in BBB cells in the absence of GB cells. The TEER value was measured using a Voltohmetro Millicell-ERS (Millipore, Billerica, MA), according to the manufacturer instructions. The mean TEER value of the plastic insert in the absence of cells was 26.73 Ω cm^2 (n=8). This value was subtracted from each value obtained in the presence of the cells.

For transport assays, after 7 days of culture, the culture medium was replaced in both chambers. 2 μM 70 kDa dextran-FITC, 2 μCi/ml [^{14}C]-sucrose, 2 μCi/ml [^{14}C]-inulin, 100 μM lucifer yellow were added to the upper chamber of Transwell. After 3 h the medium in the lower chamber was collected. The amount of [^{14}C]-sucrose and [^{14}C]-inulin was measured using a Tri-Carb Liquid Scintillation Analyzer (PerkinElmer). Radioactivity was converted in nmol/cm^2, using a calibration curve previously prepared. The radioactivity of the medium alone, considered as a blank, was subtracted from each measure.

The amount of 70 kDa dextran-FITC and lucifer yellow was measured fluorimetrically, using a Synergy HT microplate spectrofluorimeter (Bio-Tek Instruments, Winooski, VT). Excitation and emission wavelengths were: 494 nm and 518 nm (70 kDa dextran-FITC); 430 nm and 540 nm (lucifer yellow). Fluorescence was converted in nmol/cm^2, using a calibration curve previously set. The autofluorescence of the medium, considered as a blank, was subtracted from each measure. The permeability coefficients were calculated according to [36].

MDCK, Pgp-MDCK, MRP1-MDCK and BCRP-MDCK cells were a kind gift of Dr. Maria Alessandra Contino (Department of Pharmacy, University of Bari, Italy). Culturing and seeding conditions for doxorubicin transport assay were carried out as reported in [37].

GB cells. Primary human GB cells (01010627, CV17, Nov3, here identified as "patients 1, 2 and 3") were obtained from surgical samples of patients, from the Neurosurgical Unit, Universities of Torino, Italy, and Neuro-Bio-Oncology Center, Vercelli, Italy. All subjects gave their informed consent for inclusion before they participated in the study. The study was conducted in accordance with the Declaration of Helsinki, and the protocol was approved by the Ethics Committee of

Preprints (www.preprints.org) | NOT PEER-REVIEWED | Posted: 14 May 2018 doi:10.20944/preprints201805.0196.v1

Peer-reviewed version available at Molecules 2018, 23, 1401; doi:10.3390/molecules23061401

University of Torino (ORTO11WNST). The histological diagnosis was performed according to WHO guidelines. Cells were cultured as adherent cells (AC) or neurospheres (NS) as previously described [38], with minor modifications [16]. Phenotypic characterization of differentiation and stemness markers, *in vitro* clonogenicity and self-renewal, *in vivo* tumorigenicity are detailed in [16]. Morphological analysis was performed with a bright field microscope (Leica Microsystems, Wetzlar, Germany). For phenotypic characterization, the following antibodies were used: anti-nestin (Millipore), anti-CD133 (Miltenyi Biotec, Bergisch Gladbach, Germany), anti-Musashi (Millipore), anti-SOX2 (R&D Systems), anti-EGF (Cell Signaling Technology Inc, Danvers, MA), anti-p53 (Dako, Glostrup, Denmark), anti-GFAP (Dako), anti-Gal-C (Millipore), followed by goat anti-rabbit FITC-conjugated IgG and rabbit anti-mouse tetramethyl rhodamine iso-thiocyanate (TRITC)-conjugated IgG antibodies. Nuclei were counterstained with 4',6-diamidino-2-phenylindole (DAPI). The observations were made by immunofluorescence on a Zeiss Axioskop microscope equipped with an AxioCam5MRSc and coupled to an imaging system (AxixoVision Release 4.5, Zeiss), by using a 63 x oil immersion objective (1.4 numerical aperture) and 10 x ocular lens. For each experimental point, a minimum of 5 microscopic fields were examined.

In co-culture experiments, 500,000 GB cells were added in the lower chamber of Transwell devices, 4 days after seeding hCMEC/D3 cells in the Transwell insert. After 3 days of co-culture the medium of the upper and lower chamber was replaced, and cells were used for the experimental assays.

Cell viability. Cell viability was evaluated by ATPLite kit (PerkinElmer, Waltham, MA), as per manufacturer's instructions. The results were expressed as percentage of viable cells in each experimental condition versus untreated cells (considered 100%).

Immunoblotting. Cells were rinsed with ice-cold lysis buffer (50 mM, Tris, 10 mM EDTA, 1% v/v Triton-X100), supplemented with the protease inhibitor cocktail set III (80 μM aprotinin, 5 mM bestatin, 1.5 mM leupeptin, 1 mM pepstatin; Calbiochem, San Diego, CA), 2 mM

Preprints (www.preprints.org) | NOT PEER-REVIEWED | Posted: 14 May 2018 doi:10.20944/preprints201805.0196.v1

Peer-reviewed version available at Molecules 2018, 23, 1401; doi:10.3390/molecules23061401

phenylmethylsulfonyl fluoride and 1 mM Na_3VO_4, then sonicated and centrifuged at 13,000 x g for 10 min at 4°C. Twenty µg protein extracts were subjected to SDS-PAGE and probed with the following antibodies: anti-Pgp (C219; Calbiochem), anti-MRP1 (MRPm5; Abcam, UK), anti-BCRP (M-70; Santa Cruz Biotechnology Inc., Santa Cruz, CA), anti-claudin 3 (PA5-16867; ThermoFisher Scientific, Waltham, MA), anti-claudin 5 (4C3C2; ThermoFisher Scientific), anti-occludin (6HCLC; ThermoFisher Scientific), anti-ZO-1 (40-2200; ThermoFisher Scientific), anti-β-tubulin (D-10 and TUJ1; Santa Cruz Biotechnology Inc.), followed by a peroxidase-conjugated secondary antibody (Bio-Rad Laboratories). The membranes were washed with Tris-buffered saline-Tween 0.1% v/v solution, and the proteins were detected by enhanced chemiluminescence (Bio-Rad Laboratories).

Fluorescence microscopy. GB cells were seeded on sterile glass coverslips and incubated 3 h with 5 µM doxorubicin, rinsed with PBS, fixed with 4% w/v paraformaldehyde for 15 min, washed three times with PBS and incubated with DAPI for 3 min at room temperature in the dark. Cells were washed three times with PBS and once with water, then the slides were mounted with 4 µL of Gel Mount Aqueous Mounting and examined with a Leica DC100 fluorescence microscope (Leica Microsystems GmbH, Wetzlar, Germany). For each experimental point, a minimum of 5 microscopic fields were examined.

Doxorubicin uptake. hCMEC/D3 cells, grown up to confluence for 7 days in Transwell devices, or GB cells were incubated 3 h with 5 µM doxorubicin, washed with PBS, trypsinized and centrifuged at 13,000 x g for 5 min and re-suspended in 0.5 mL of 1/1 solution ethanol/0.3 N HCl. A 50 µL aliquot was taken away, sonicated and used for the measurement of the protein content. The intracellular fluorescence of doxorubicin was measured spectrofluorimetrically, using a Synergy HT microplate spectrofluorimeter (Bio-Tek Instruments). Excitation and emission wavelengths were 475 nm and 553 nm. Fluorescence was converted in nmol/mg cell proteins, using a calibration curve previously set. The intratumor doxorubicin delivery to GB grown under BBB monolayer was

Preprints (www.preprints.org) | NOT PEER-REVIEWED | Posted: 14 May 2018 doi:10.20944/preprints201805.0196.v1

Peer-reviewed version available at Molecules 2018, 23, 1401; doi:10.3390/molecules23061401

measured as previously described [11]. After 3 days of co-culture, 5 µM doxorubicin, alone or in the presence of the compounds, was added to the upper chamber of Transwell inserts containing hCMEC/D3 cells monolayer. After 3 h, GB cells were collected from the lower chamber and the intracellular amount of doxorubicin was measured spectrofluorimetrically as described above.

Cytotoxicity. The release of LDH in cell supernatant was measured as reported in [16], using a Synergy HT microplate reader. Both intracellular and extracellular enzyme activities were expressed as µmol NADH oxidized/min/dish, then extracellular LDH activity was calculated as percentage of the total LDH activity. For cytotoxicity assays in co-cultures, 5 µM doxorubicin, alone or in the presence of compounds, was added to the upper chamber of Transwell inserts. After 24 h, both cell culture medium and GB cells from the lower chamber were collected, and checked for the activity of LDH, as described above.

Caspase 3 activity. The activity of caspase 3, taken as an index of apoptosis, was measured by incubating 20 µg cell lysates, collected from GB cells or GB cells growing under BBB monolayer, as reported above, with the fluorogenic substrate DEVD-7-amino-4-methylcumarine (DEVD-AMC), as reported [11]. Results were expressed as nmoles AMC/mg proteins, using a calibration curve previously set.

Statistical analysis. All data in the text and figures are provided as means ± SD. The results were analyzed by a one-way analysis of variance (ANOVA) and Tukey's test. $p < 0.05$ was considered significant.

Supplementary Materials

Supplementary Figure 1. Effects of Pgp ligands on mitoxantrone permeability across BBB

Supplementary Figure 2. Effects of MRP1 and BCRP inhibitors on doxorubicin transport across BBB

Supplementary Figure 3. Effects of Pgp ligands on doxorubicin transport on Pgp-MDCK, MRP1-MDCK and BCRP-MDCK cells

Supplementary Figure 4. Effects of Pgp ligands on dextran, sucrose, inulin and lucifer yellow permeability across BBB

Supplementary Table 1. Phenotypic characterization of cells from patient number 1, 2, 3 by immunofluorescence analysis

Acknowledgments

This work was supported with funds from Italian Ministry of University and Research (Future in Research - FIRB 2012, grant RBFR12SOQ1 to CR) and from University of Turin, "Ricerca locale - ex 60%". The funding institutions had no role in the study design, data collection and analysis, or in writing the manuscript.

We would like to thank prof. Alberto Gasco for the fruitful discussions.

Author Contributions

SG and KC synthesized and characterized the compounds; ICS, CC, EG and JK performed the in vitro experiments, and analyzed the data; FR, SG and CR conceived and supervised the work, wrote and revised the manuscript. All authors approved the submitted version.

Conflicts of Interest

The authors declare there are no conflict of interest.

References

1. Ellor, S.V.; Pagano-Young, T.A.; Avgeropoulos, N.G. Glioblastoma: background, standard treatment paradigms, and supportive care considerations. *J Law Med Ethics* **2014**, *42*, 171-82. DOI: 10.1111/jlme.12133. Available online:

Peer-reviewed version available at *Molecules* **2018**, *23*, 1401; doi:10.3390/molecules23061401

http://journals.sagepub.com/doi/abs/10.1111/jlme.12133?url_ver=Z39.88-2003&rfr_id=ori%3Arid%3Acrossref.org&rfr_dat=cr_pub%3Dpubmed& (accessed on 09 12 2017)

2. Bai, R.Y.; Staedke, V.; Riggins, G.J. Molecular targeting of GBM: Drug discovery and therapies. *Trends Mol Med* **2011**, *17*, 301-12. DOI: 10.1016/j.molmed.2011.01.011. Available online: http://www.cell.com/trends/molecular-medicine/fulltext/S1471-4914(11)00012-8?_returnURL=http%3A%2F%2Flinkinghub.elsevier.com%2Fretrieve%2Fpii%2FS1471491411000128%3Fshowall%3Dtrue (accessed on 09 12 2017)

3. Beier, D.; Schulz, J.B.; Beier, C.P. Chemoresistance of glioblastoma cancer stem cells--much more complex than expected. *Mol Cancer* **2011**, *10*, e128. DOI: 10.1186/1476-4598-10-128. Available online: https://molecular-cancer.biomedcentral.com/articles/10.1186/1476-4598-10-128 (accessed on 06 11 2017)

4. Corso, C.D.; Bindra, R.S. Success and Failures of Combined Modalities in Glioblastoma Multiforme: Old Problems and New Directions. *Semin Radiat Oncol* **2016**, *26*, 281-98. DOI: 10.1016/j.semradonc.2016.06.003. Available online: http://www.semradonc.com/article/S1053-4296(16)30018-2/fulltext (accessed on 10 12 2017)

5. Salmaggi, A.; Boiardi, A.; Gelati, M.; Russo, A.; Calatozzolo, C.; Ciusani, E.; Sciacca, F.L.; Ottolina, A.; Parati, E.A.; La Porta, C.; Alessandri, G.; Marras, C.; Croci, D.; De Rossi, M. GBM-Derived Tumorospheres Identify a Population of Tumor Stem-Like Cells with Angiogenic Potential and Enhanced Multidrug Resistance Phenotype. *Glia* **2006**, *54*, 850-60. DOI: 10.1002/glia.20414. Available online: http://onlinelibrary.wiley.com/doi/10.1002/glia.20414/abstract;jsessionid=16A8F24E7BD156C3CC3BCF5B3ED708AC.f02t02 (accessed on 10 12 2017)

6. Auffinger, B.; Spencer, D.; Pytel, P.; Ahmed, A.U.; Lesniak, M.S. The role of glioma stem cells in chemotherapy resistance and glioblastoma multiforme recurrence. *Expert Rev Neurother*. **2015**, *15*, 741-52. DOI: 10.1586/14737175.2015.1051968. Available online:

http://www.tandfonline.com/doi/abs/10.1586/14737175.2015.1051968?journalCode=iern20 (accessed on 9 12 2017)

7. Agarwal, S.; Sane, R.; Oberoi, R.; Ohlfest, J.R.; Elmquist, W.F. Delivery of molecularly targeted therapy to malignant glioma, a disease of the whole brain. *Expert Rev Mol Med* **2011**, **1**3, e17. DOI: 10.1017/S1462399411001888. Available online: https://www.cambridge.org/core/journals/expert-reviews-in-molecular-medicine/article/delivery-of-molecularly-targeted-therapy-to-malignant-glioma-a-disease-of-the-whole-brain/45B082815504D678D70CAB70E3AABB0F (accessed on 13 02 2016)

8. Pinzón-Daza, M.L.; Campia, I.; Kopecka, J.; Garzón, R.; Ghigo, D.; Riganti, C. Nanoparticle- and liposome-carried drugs: new strategies for active targeting and drug delivery across blood-brain barrier. *Curr Drug Metab* **2013**, *14*, 625-40. DOI: 10.2174/1389200211314060001. Available online: http://www.eurekaselect.com/112973/article (accessed on 06 06 2015)

9. Zhou, Y.G.; Li, K.Y.; Li, H.D. Effect of the novel antipsychotic drug perospirone on P-glycoprotein function and expression in Caco-2 cells. *Eur J Clin Pharmacol*. **2008**, *64*, 697-703. DOI: 10.1007/s00228-008-0487-5. Available online: https://link.springer.com/article/10.1007%2Fs00228-008-0487-5 (accessed on 09 12 2017)

10. Bauer, F.; Wanek, T.; Mairinger, S.; Stanek, J.; Sauberer, M.; Kuntner, C.; Parveen, Z.; Chiba, P.; Müller, M.; Langer, O; Erker, T. Interaction of HM30181 with P-glycoprotein at the murine blood-brain barrier assessed with positron emission tomography. *Eur J Pharmacol*. **2012**, *696*, 18-27. DOI: 10.1016/j.ejphar.2012.09.013. Available online: http://www.sciencedirect.com/science/article/pii/S0014299912007674?via%3Dihub (accessed on 09 12 2017)

11. Pinzón-Daza, M.; Garzón, R.; Couraud, P.; Romero, I; Weksler, B.; Ghigo, D.; Bosia, A.; Riganti, C. The association of statins plus LDL receptor-targeted liposome-encapsulated doxorubicin increases in vitro drug delivery across blood-brain barrier cells. *Br J Pharmacol* **2012**, *167*, 1431-47. DOI: 10.1111/j.1476-5381.2012.02103.x. Available online:

http://onlinelibrary.wiley.com/doi/10.1111/j.1476-5381.2012.02103.x/epdf (accessed on 27 11 2014)

12. Riganti, C.; Salaroglio, I.C.; Pinzòn-Daza, M.L.; Caldera, V.; Campia, I.; Kopecka, J.; Mellai, M.; Annovazzi, L.; Couraud, P.O.; Bosia, A.; Ghigo, D.; Schiffer, D. Temozolomide down-regulates P-glycoprotein in human blood-brain barrier cells by disrupting Wnt3 signaling. *Cell Mol Life Sci* **2014**, *71*, 499-516. DOI: 10.1007/s00018-013-1397-y. Available online: https://link.springer.com/article/10.1007%2Fs00018-013-1397-y (accessed on 01 09 2015)

13. Pinzón-Daza, M.L.; Salaroglio, I.C.; Kopecka, J.; Garzòn, R.; Couraud, P.O.; Ghigo, D.; Riganti, C. The cross-talk between canonical and non-canonical Wnt-dependent pathways regulates P-glycoprotein expression in human blood-brain barrier cells. *J Cereb Blood Flow Metab* 2014, 34, 1258-69. DOI: 10.1038/jcbfm.2014.100. Available online: http://journals.sagepub.com/doi/pdf/10.1038/jcbfm.2014.100 (accessed on 17 08 2014)

14. Bauer, M.; Karch, R.; Zeitlinger, M.; Philippe, C.; Römermann, K.; Stanek, J.; Maier-Salamon, A.; Wadsak, W.; Jäger, W.; Hacker, M.; Müller, M.; Langer, O. Approaching complete inhibition of P-glycoprotein at the human blood-brain barrier: an (R)-[^{11}C]verapamil PET study. *J Cereb Blood Flow Metab* **2015**, *35*, 743-6. DOI: 10.1038/jcbfm.2015.19. Available online: http://journals.sagepub.com/doi/pdf/10.1038/jcbfm.2015.19 (accessed on 10 12 2017)

15. Agarwal, S.; Mittapalli, R.K.; Zellmer, D.M.; Gallardo, J.L.; Donelson, R.; Seiler, C.; Decker, S.A.; SantaCruz, K.S.; Pokorny, J.L.; Sarkaria, J.N.; Elmquist, W.F.; Ohlfest, J.R. Active efflux of dasatinib from the brain limits efficacy against murine glioblastoma: broad implications for the clinical use of molecularly-targeted agents. *Mol Cancer Ther* **2012**, *11*, 2183-92. DOI: 10.1158/1535-7163.MCT-12-0552. Available online: http://mct.aacrjournals.org/content/11/10/2183.full-text.pdf (accessed on 10 12 2017)

16. Riganti, C.; Salaroglio, I.C.; Caldera, V.; Campia, I.; Kopecka, J.; Mellai, M.; Annovazzi, L.; Bosia, A.; Ghigo, D.; Schiffer, D. Temozolomide downregulates P-glycoprotein expression in glioblastoma stem cells by interfering with the Wnt3a/glycogen synthase-3 kinase/β-catenin

pathway. *Neuro Oncol* **2013**, *15*, 1502-17. DOI: 10.1093/neuonc/not104. Available online: https://academic.oup.com/neuro-oncology/article/15/11/1502/1051109 (accessed on 16 06 2014)

17. Sheehy, R.M.; Kuder, C.H.; Bachman, Z.; Hohl, R.J. Calcium and P-glycoprotein independent synergism between schweinfurthins and verapamil. *Cancer Biol Ther* **2015**, *16*, 1259-68. DOI: 10.1080/15384047.2015.1056420. Available online: http://www.tandfonline.com/doi/pdf/10.1080/15384047.2015.1056420?needAccess=true (accessed on 10 12 2017)

18. Guglielmo, S.; Lazzarato, L.; Contino, M.; Perrone, M.G.; Chegaev, K.; Carrieri, A.; Fruttero, R.; Colabufo, N.A.; Gasco, A. Structure-Activity Relationship Studies on Tetrahydroisoquinoline Derivatives: [4'-(6,7-Dimethoxy-3,4-dihydro-1H-isoquinolin-2-ylmethyl)biphenyl-4-ol] (MC70) Conjugated through Flexible Alkyl Chains with Furazan Moieties Gives Rise to Potent and Selective Ligands of P-glycoprotein. *J Med Chem* **2016**, *59*, 6729-38. DOI: 10.1021/acs.jmedchem.6b00252. Available online: http://pubs.acs.org/doi/pdf/10.1021/acs.jmedchem.6b00252 (accessed on 10 12 2017)

19. Guglielmo, S.; Contino, M.; Lazzarato, L.; Perrone, M.G.; Blangetti, M.; Fruttero, R.; Colabufo, N.A. A Potent and Selective P-gp Modulator for Altering Multidrug Resistance Due to Pump Overexpression. *ChemMedChem.* **2016**, *11*, 374-6. DOI: 10.1002/cmdc.201500538. Available online: http://onlinelibrary.wiley.com/doi/10.1002/cmdc.201500538/pdf (accessed on 10 12 2017)

20. Colabufo, N.A.; Berardi, F.; Cantore, M.; Perrone, M.G.; Contino, M.; Inglese, C.; Niso, M.; Perrone, R.; Azzariti, A.; Simone, G. M.; Paradiso, A. 4-Biphenyl and 2-naphthyl substituted 6,7-dimethoxytetrahydroisoquinoline derivatives as potent P-gp modulators. *Bioorg. Med. Chem.* **2008**, *16*, 3732-43. DOI: 10.1016/j.bmc.2008.01.055. Available online: https://www.sciencedirect.com/science/article/pii/S0968089608000916?via%3Dihub accessed on 10 12 2017)

21. Akhtar, N.; Ahad, A.; Khar, R.K.; Jaggi, M.; Aqil, M.; Iqbal, Z.; Ahmad, F.J.; Talegaonkar, S. The emerging role of P glycoprotein inhibitors in drug delivery: a patent review. *Expert Opin Ther*

Pat 2011, 21, 561-76. DOI: 10.1517/13543776.2011.561784. Available online: http://www.tandfonline.com/doi/full/10.1517/13543776.2011.561784?needAccess=true (accessed on 10 12 2017)

22. Weksler, B.B.; Subileau, E.A.; Perrière, N.; Charneau, P.; Holloway, K.; Leveque, M.; Tricoire-Leignel, H.; Nicotra, A.; Bourdoulous, S.; Turowski, P.; Male, D.K.; Roux, F.; Greenwood, J.; Romero, I.; Couraud, P.O. Blood-brain barrier-specific properties of a human adult brain endothelial cell line. *FASEB J* **2005**, *19*, 1872-94. DOI: 10.1096/fj.04-3458fje. Available online: http://www.fasebj.org/content/early/2005/11/01/fj.04-3458fje.long (accessed on 11 08 2010)

23. Monnaert, V.; Betbeder, D.; Fenart, L.; Bricout, H.; Lenfant, A.M.; Landry, C.; Cecchelli, R.; Monflier, E.; Tilloy, S. Effects of γ- and hydroxypropyl- γ -cyclodextrins on the transport of doxorubicin across an in vitro model of blood-brain barrier. *J Pharmacol Exp Ther* **2004**, *311*, 1115-20. DOI: 10.1124/jpet.104.071845. Available online: http://jpet.aspetjournals.org/content/jpet/311/3/1115.full.pdf (accessed on 18 09 2011)

24. Yang, S.; Mei, S.; Jin, H.; Zhu, B.; Tian, Y.; Huo, J.; Cui, X.; Guo, .; Zhao, Z. Identification of two immortalized cell lines, ECV304 and bEnd3, for in vitro permeability studies of blood-brain barrier. *PLoS One*. **2017**, *12,* e0187017. DOI: 10.1371/journal.pone.0187017. Available online: http://journals.plos.org/plosone/article?id=10.1371/journal.pone.0187017 (accessed on 25 02 2018)

25. Callaghan, R.; Luk, F.; Bebawy, M. Inhibition of the multidrug resistance P-glycoprotein: time for a change of strategy? *Drug Metab Dispos* **2014**, *42*, 623-31. DOI: 10.1124/dmd.113.056176. Available online: http://dmd.aspetjournals.org/content/dmd/42/4/623.full.pdf (accessed on 21 03 2015)

26. Szakács, G.; Hall, M.D.; Gottesman, M.M.; Boumendiel, A.; Kachadourian, R.; Day, B.J.; Baubichon-Cortay, H.; Di Pietro, A. Targeting the Achilles Heel of Multidrug-Resistant Cancer by Exploiting the Fitness Cost of Resistance. *Chem. Rev.* **2014**, *114*, 5753-74. DOI: 10.1021/cr4006236. Available online: http://pubs.acs.org/doi/pdf/10.1021/cr4006236 (accessed on 24 03 2015)

Peer-reviewed version available at *Molecules* **2018**, *23*, 1401; doi:10.3390/molecules23061401

27. Chen, Z.; Shi, T.; Zhang, L.; Zhu, P.; Deng, M.; Huang, C.; Hu, T.; Jiang, L.; Li, J. Mammalian drug efflux transporters of the ATP binding cassette(ABC) family in multidrug resistance: A review of the past decade. *Cancer Lett* **2016**, *370*, 153-64. DOI: 10.1016/j.canlet.2015.10.010. Available online: http://www.cancerletters.info/article/S0304-3835(15)00627-8/pdf (accessed on 28 12 2017)

28. Pan, A.C.; Borhani, D.W.; Dror, R.O.; Shaw, D.E. Molecular determinants of drug–receptor binding kinetics. *Drug Discovery Today*. **2013**, *18*, 667-673. DOI: 10.1016/j.drudis.2013.02.007. Available online: https://www.sciencedirect.com/science/article/pii/S1359644613000627?via%3Dihub (accessed on 01 03 2018)

29. Martin, C.; Berridge, G.; Higgins, C.F.; Mistry, P.; Charlton, P.; Callaghan, R. Communication between multiple drug binding sites on P-glycoprotein. *Mol Pharmacol*. **2000**, *58*, 624-632. DOI: https://doi.org/10.1124/mol.58.3.624. Available online: http://molpharm.aspetjournals.org/content/molpharm/58/3/624.full.pdf (accessed on 30 04 2018).

30. Tai, L.M.; Sreekanth Reddy, P.; Lopez-Ramirez, A.M.; Davies, H.A.; Male, A.D.K.; Loughlin, A.J; Romero, I.A. Polarized P-glycoprotein expression by the immortalized human brain endothelial cell line, hCMEC/D3, restricts apical-to-basolateral permeability to rhodamine 123. *Brain Res* **2009**, 1292, 14-24. DOI: https://www.sciencedirect.com/science/article/pii/S0006899309014735?via%3Dihub (accessed online on 08 03 2018)

31. Hau, P.; Fabel, K.; Baumgart, U.; Rümmele, P.; Grauer, O.; Bock, A.; Dietmaier, C.; Dietmaier, W.; Dietrich, J.; Dudel, C.; Hübner, F.; Jauch, T.; Drechsel, E.; Kleiter, I.; Wismeth, C.; Zellner, A.; Brawanski, A.; Steinbrecher, A.; Marienhagen, J.; Bogdahn, U. Pegylated liposomal doxorubicin-efficacy in patients with recurrent high-grade glioma. *Cancer* 2004, 100, 1199-207. DOI: 10.1002/cncr.20073. Available online: http://onlinelibrary.wiley.com/doi/10.1002/cncr.20073/epdf (accessed on 03 01 2011)

32. Kovacs, Z.; Werner, B.; Rassi, A.; Sass, J.O.; Martin-Fiori, E.; Bernasconi, M. Prolonged survival upon ultrasound-enhanced doxorubicin delivery in two syngenic glioblastoma mouse models. *J Control Release* **2014**, *187*, 74-82. DOI: 10.1016/j.jconrel.2014.05.033. Available online: http://www.sciencedirect.com/science/article/pii/S0168365914003368?via%3Dihub (accessed on 27 12 2017)

33. Mita, M.M.; Natale, R.B.; Wolin, E.M.; Laabs, B.; Dinh, H.; Wieland, S.; Levitt, D.J.; Mita, A.C. Pharmacokinetic study of aldoxorubicin in patients with solid tumors. *Invest New Drugs* **2015**, *33*, 341-8. DOI: 10.1007/s10637-014-0183-5. Available online: https://link.springer.com/content/pdf/10.1007%2Fs10637-014-0183-5.pdf (accessed on 27 12 2017)

34. Whittle, J.R.; Lickliter, J.D.; Gan, H.K.; Scott, A.M.; Simes, J.; Solomon, B.J.; MacDiarmid, J.A.; Brahmbhatt, H.; Rosenthal, M.A. First in human nanotechnology doxorubicin delivery system to target epidermal growth factor receptors in recurrent glioblastoma. *J Clin Neurosci* **2015**, *22,* 1889-94. DOI: 10.1016/j.jocn.2015.06.005. Available online: http://www.jocn-journal.com/article/S0967-5868(15)00317-3/pdf (accessed on 27 12 2017)

35. Munoz, J.L.; Walker, N.D.; Scotto, K.W.; Rameshwar, P. Temozolomide competes for P-glycoprotein and contributes to chemoresistance in glioblastoma cells. *Cancer Lett* **2015,** *367*, 69-75. DOI: 10.1016/j.canlet.2015.07.013. Available online: http://www.cancerletters.info/article/S0304-3835(15)00455-3/pdf (accessed on 27 12 2017)

36. Siflinger-Birnboim, A.; Del Vecchio, P.J.; Cooper, J.A.; Blumenstock, F.A.; Shepard, J.M.; Malik, A.B. Molecular sieving characteristics of the cultured endothelial monolayer. *J Cell Physiol* **1987**, *132*, 111-117. DOI: 10.1002/jcp.1041320115. Available online: http://onlinelibrary.wiley.com/doi/10.1002/jcp.1041320115/pdf (accessed on 03 05 2010)

37. Kuteykin-Teplyakov, K.; Luna-Tortós, C.; Ambroziak, K.; Löscher, W. Differences in the expression of endogenous efflux transporters in MDR1-transfected versus wildtype cell lines affect P-glycoprotein mediated drug transport. *Br J Pharmacol* **2010,** *160*, 1453-63. DOI: 10.1111/j.1476-5381.2010.00801. Available online:

https://bpspubs.onlinelibrary.wiley.com/doi/epdf/10.1111/j.1476-5381.2010.00801.x (accessed on 26 04 2018)

38. Reynolds, B.A.; Tetzlaff, W.; Weiss, S. A multipotent EGF-responsive striatal embryonic progenitor cell produces neurons and astrocytes. *J Neurosci* **1992**, *12,* 4565-74. Available online: http://www.jneurosci.org/content/jneuro/12/11/4565.full.pdf (accessed on 09 08 2011)

Figure legends

Preprints (www.preprints.org) | NOT PEER-REVIEWED | Posted: 14 May 2018 doi:10.20944/preprints201805.0196.v1

Peer-reviewed version available at Molecules 2018, 23, 1401; doi:10.3390/molecules23061401

Figure 1

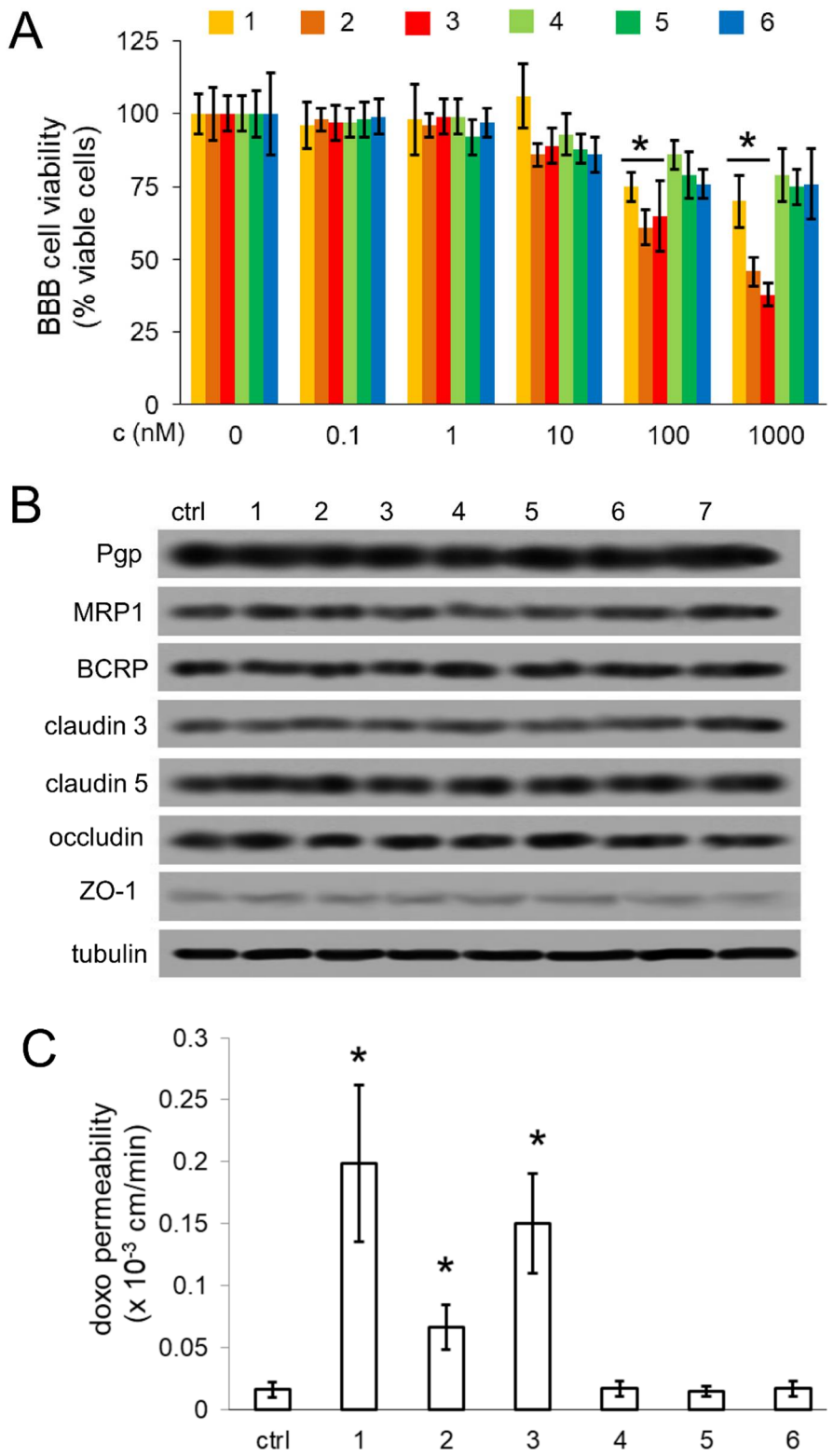

Figure 1. Effects of Pgp ligands of BBB viability and integrity

A. hCMEC/D3 cells were grown in the upper insert of Transwell devices for 7 days. The medium was then replaced with fresh medium (0) or with medium containing compounds **1-6** at the

Preprints (www.preprints.org) | NOT PEER-REVIEWED | Posted: 14 May 2018 doi:10.20944/preprints201805.0196.v1

Peer-reviewed version available at *Molecules* **2018**, *23*, 1401; doi:10.3390/molecules23061401

indicated concentrations for 24 h. Cell viability was measured by a chemiluminescence-based assay, in triplicates. Data are presented as means ± SD (n = 4). Versus untreated (0) cells: * $p < 0.05$. **B.** hCMEC/D3 cells were grown in the upper insert of Transwell devices for 7 days. The medium was then replaced with fresh medium (ctrl) or with medium containing 1 nM of compounds **1-6** for 24 h. Cells were lysed and immunoblotted with the indicated antibodies. β-tubulin level was used as control of equal protein loading. The figure is representative of one out of three experiments with similar results. **C.** Cells were grown in the upper insert of Transwell devices and incubated as indicated in **B**. 5 µM doxorubicin (doxo) was added during the last 3 h. The amount of doxorubicin in the medium of the lower chamber was measured spectrofluorimetrically, in duplicates. Data are presented as means ± SD (n = 4). Versus dox: * $p < 0.005$.

Preprints (www.preprints.org) | NOT PEER-REVIEWED | Posted: 14 May 2018 doi:10.20944/preprints201805.0196.v1

Peer-reviewed version available at Molecules 2018, 23, 1401; doi:10.3390/molecules23061401

Figure 2

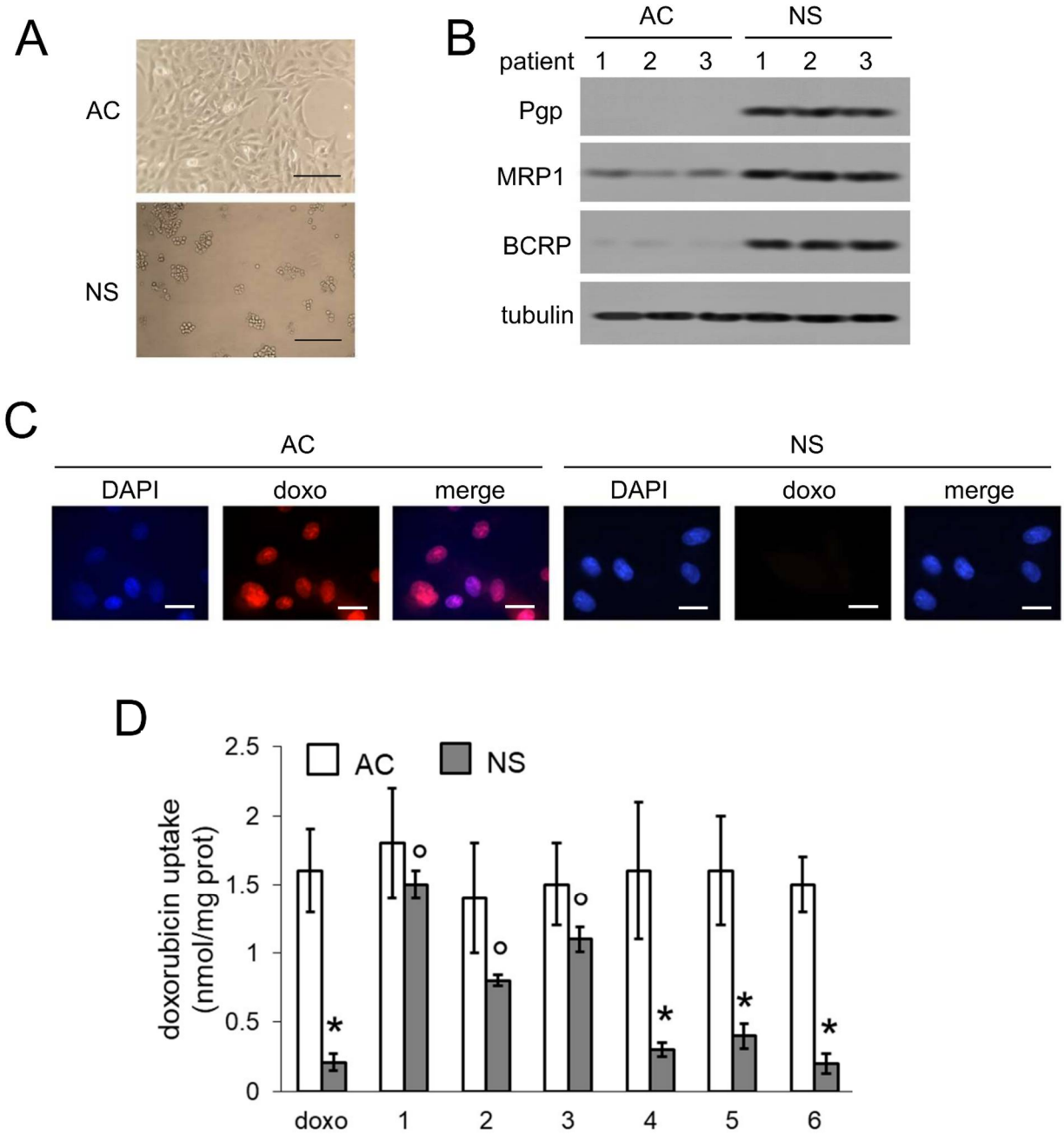

Figure 2. Effects of Pgp ligands on doxorubicin retention of glioblastoma cells

A. Representative bright field microscope images of glioblastoma cells, cultured as adherent cells (AC) or neurospheres (NS). Magnification: 60 × objective (0.52 numerical aperture); 10 × ocular lens. Bar: 20 µm. The micrographs are representative of patient 2. No significant differences in cell morphology were detected for patient 1 and 3. **B.** AC or NS from each patient were lysed and

Preprints (www.preprints.org) | NOT PEER-REVIEWED | Posted: 14 May 2018 doi:10.20944/preprints201805.0196.v1

Peer-reviewed version available at *Molecules* **2018**, *23*, 1401; doi:10.3390/molecules23061401

immunoblotted with the indicated antibodies. β-tubulin level was used as control of equal protein loading. The figure is representative of one out of three experiments with similar results. **C.** AC and NS from patient 2 were seeded on sterile glass coverslips, incubated 3 h with 5 µM doxorubicin (doxo), then stained with DAPI and analyzed by fluorescence microscopy to detect the intracellular accumulation of the drug. Magnification: 63 x objective (1.4 numerical aperture); 10 x ocular lens. The micrographs are representative of three experiments with similar results. No significant differences were detected for patient 1 and 3. Bar: 5 µm. **D.** AC and NS were incubated for 3 h with 5 µM doxorubicin (doxo), in the absence or presence of 1 nM of compounds **1-6**. The intracellular doxorubicin was quantified fluorimetrically, in duplicates. Pooled data of patients 1-3 are presented as means ± SD (n = 3). Vs AC doxo: * $p < 0.001$; vs NS doxo: ° $p < 0.001$.

Preprints (www.preprints.org) | NOT PEER-REVIEWED | Posted: 14 May 2018 doi:10.20944/preprints201805.0196.v1

Peer-reviewed version available at *Molecules* **2018**, *23*, 1401; doi:10.3390/molecules23061401

Figure 3

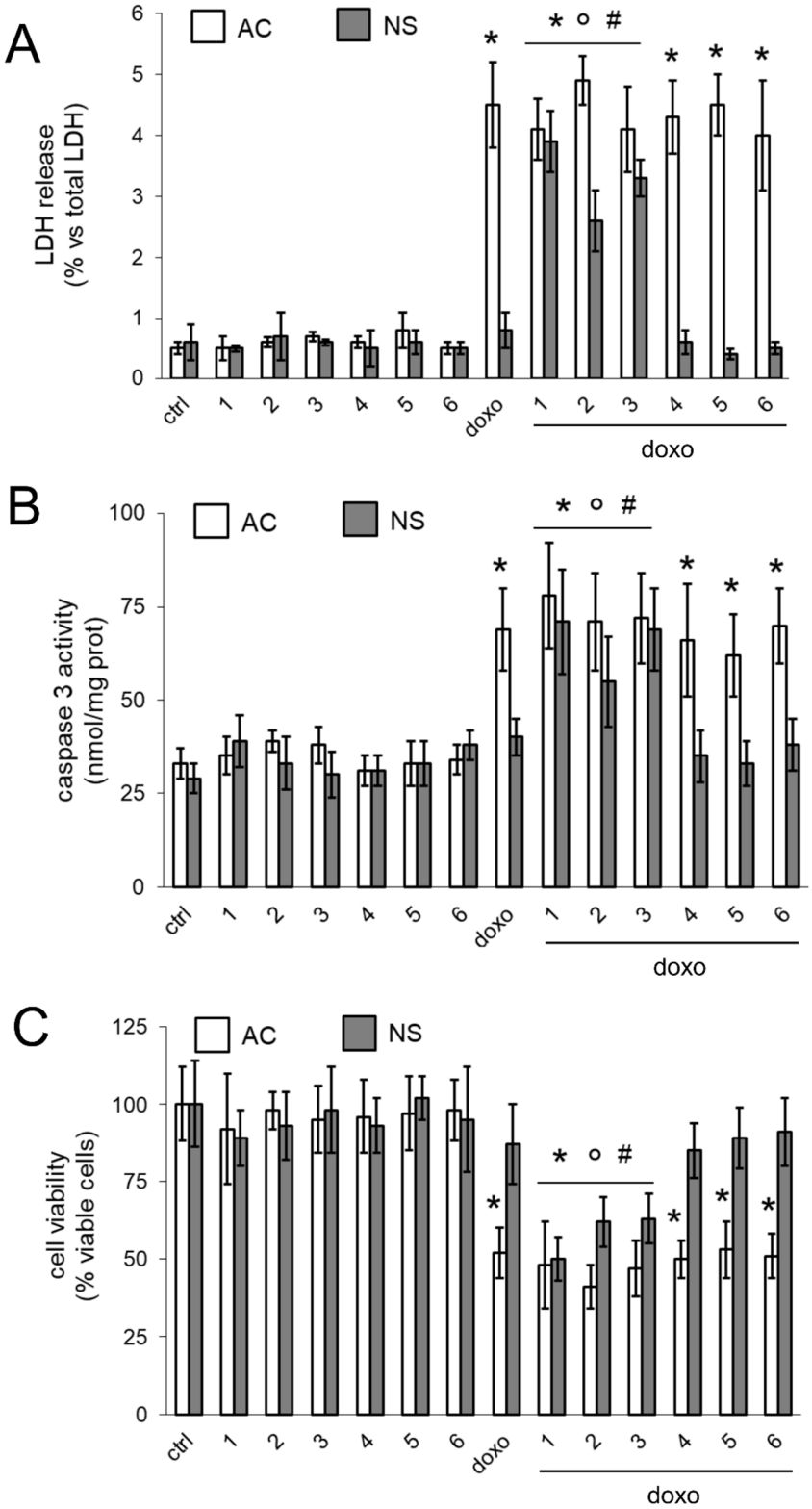

Figure 3. Effects of Pgp ligands on doxorubicin cytotoxicity in glioblastoma cells

Adherent cells (AC) or neurospheres (NS) from glioblastoma samples were grown 24 h (panel **A-B**) or 48 h (panel **C**) in fresh medium (ctrl) or in the presence of 1 nM of compounds **1-6**. When

Preprints (www.preprints.org) | NOT PEER-REVIEWED | Posted: 14 May 2018 doi:10.20944/preprints201805.0196.v1

Peer-reviewed version available at Molecules 2018, 23, 1401; doi:10.3390/molecules23061401

indicated, 5 µM doxorubicin (doxo) was co-incubated. **A.** The cell culture supernatant was checked spectrophotometrically for the extracellular activity of LDH, in duplicates. Pooled data of patients 1-3 are presented as means ± SD (n= 3). Vs AC ctrl: * $p < 0.001$; vs NS ctrl: ° $p < 0.001$; vs NS doxo: # $p < 0.001$. **B.** The activity of caspase 3 was measured fluorimetrically, in duplicates. Data are means ± SD (n=3). Pooled data of patients 1-3 are presented as means ± SD (n= 3). Vs AC ctrl: * $p < 0.001$; vs NS ctrl: ° $p < 0.01$; vs NS doxo: # $p < 0.05$. **C.** Cell viability was measured by a chemiluminescence-based assay, in quadruplicates. Pooled data of patients 1-3 are presented as means ± SD (n= 3). Vs AC ctrl: * $p < 0.001$; vs NS ctrl: ° $p < 0.001$; vs NS doxo: # $p < 0.005$.

Figure 4

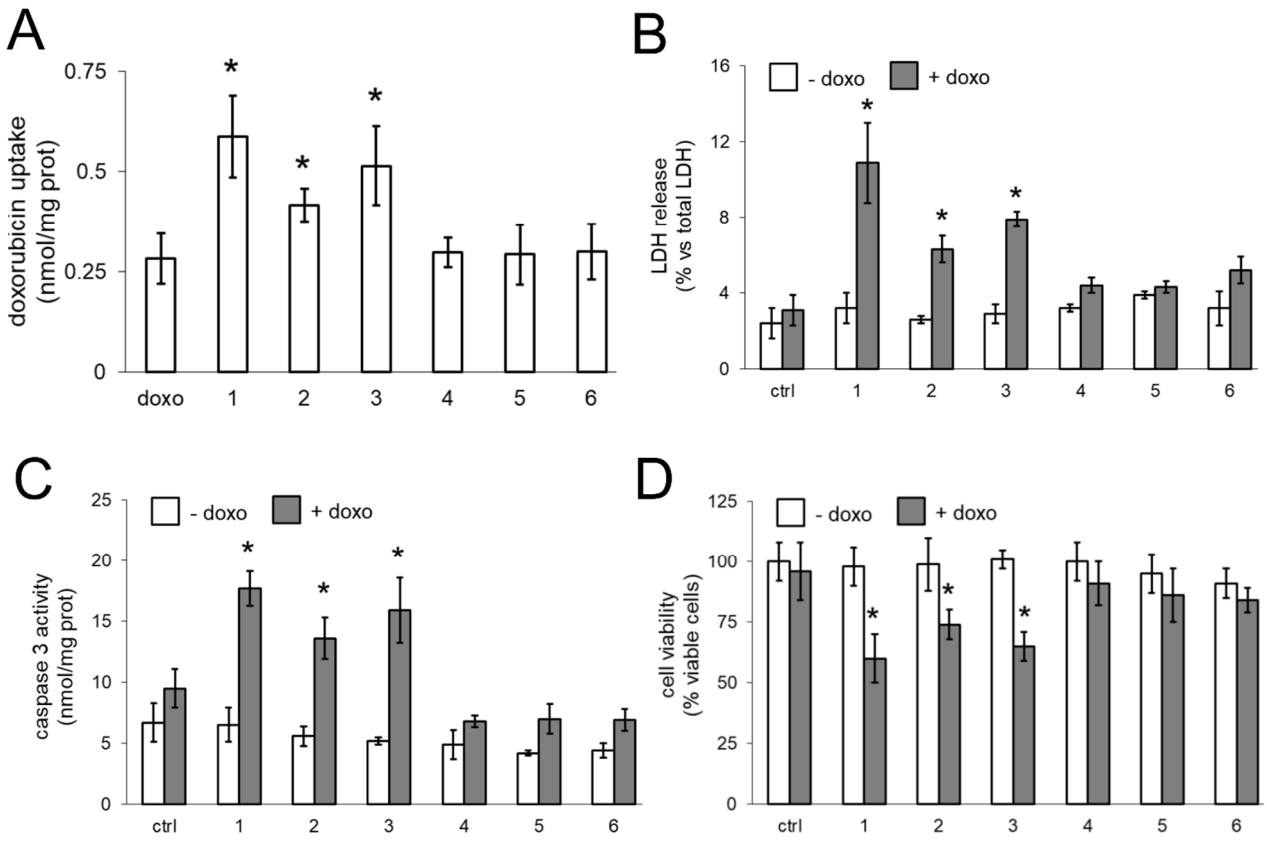

Figure 4. Effects of Pgp ligands on doxorubicin delivery and cytotoxicity in BBB-glioblastoma cells co-cultures

Preprints (www.preprints.org) | NOT PEER-REVIEWED | Posted: 14 May 2018 doi:10.20944/preprints201805.0196.v1

Peer-reviewed version available at *Molecules* **2018**, *23*, 1401; doi:10.3390/molecules23061401

hCMEC/D3 cells were grown for 7 days up to confluence in Transwell inserts; neurospheres (NS) were seeded at day 4 in the lower chamber. After 3 days of co-culture, supernatant in the upper chamber was replaced with fresh medium (ctrl) or with medium containing 5 µM doxorubicin (doxo), in the absence (ctrl) or presence of 1 nM of compounds **1-6**. **A**. Fluorimetric quantification of intracellular doxorubicin in NS after 6 h. Pooled data of patients 1-3 are presented as means ± SD (n = 3). Vs doxo: * $p < 0.01$. **B.** The culture supernatant of NS was checked spectrophotometrically for the extracellular activity of LDH after 24 h. Pooled data of patients 1-3 are presented as means ± SD (n= 3). Vs untreated cells (ctrl, either "-doxo" or "+doxo"): * $p < 0.001$. **C.** The activity of caspase 3 was measured fluorimetrically in NS lysates after 24 h, in duplicates. Pooled data of patients 1-3 are presented as means ± SD (n= 3). Vs untreated cells (ctrl, either "-doxo" or "+doxo"): * $p < 0.002$. **D.** Cell viability of NS was measured after 48 h by a chemiluminescence-based assay, in quadruplicates. Pooled data of patients 1-3 are presented as means ± SD (n= 3). Vs untreated cells (ctrl, either "-doxo" or "+doxo"): * $p < 0.02$.

Preprints (www.preprints.org) | NOT PEER-REVIEWED | Posted: 14 May 2018 doi:10.20944/preprints201805.0196.v1

Peer-reviewed version available at Molecules 2018, 23, 1401; doi:10.3390/molecules23061401

Figure 5

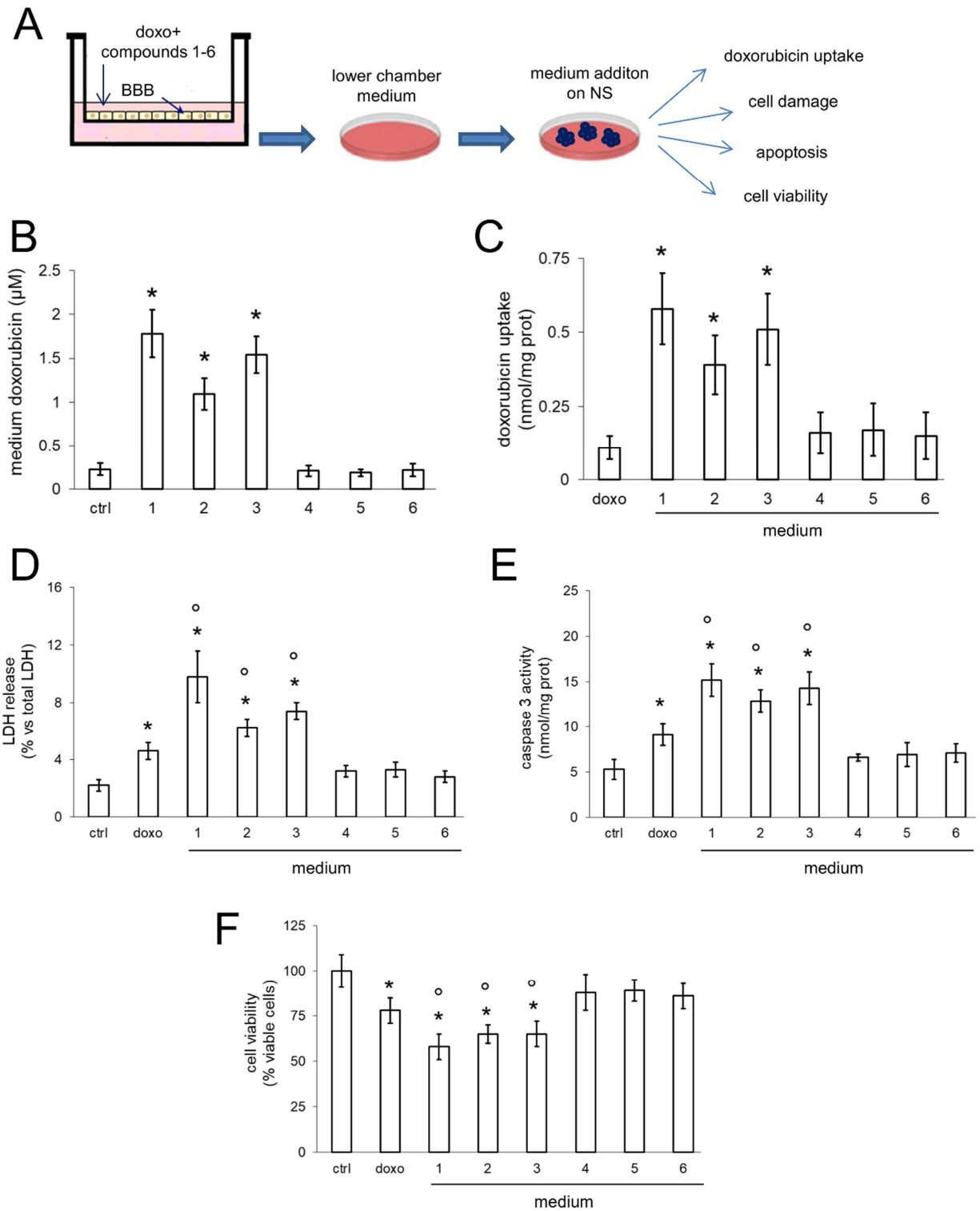

743

744 **Figure 5. Possible dual effects of Pgp ligands on Pgp on BBB and glioblastoma cells**

Preprints (www.preprints.org) | NOT PEER-REVIEWED | Posted: 14 May 2018 doi:10.20944/preprints201805.0196.v1

Peer-reviewed version available at *Molecules* **2018**, *23*, 1401; doi:10.3390/molecules23061401

A. hCMEC/D3 cells were grown for 7 days up to confluence in Transwell inserts, then the supernatant in the upper chamber was replaced with fresh medium (ctrl) or with medium containing 5 µM doxorubicin, in the absence (ctrl) or presence of 1 nM of compounds **1-6**. After 3 h the medium of the lower chamber was removed and added to neuropsheres (NS) for the measure of intracellular doxorubicin uptake, LDH release, caspase-3 activity and cell viability (panels **C-F**). In all these panels, a standard solution of 1 µM doxorubicin (doxo) was used as internal control. **B.** Fluorimetric quantification of doxorubicin in the medium of the lower chamber incubated as reported in **A.** Data are means ± SD (n = 3). Vs ctrl: * $p < 0.001$. **C**. Fluorimetric quantification of intracellular doxorubicin in NS after 6 h, treated with 1 µM doxorubicin (doxo) or with media of the lower chamber containing 5 µM doxorubicin+compounds **1-6**. Pooled data of patients 1-3 are presented as means ± SD (n = 3). Vs doxo: * $p < 0.001$. **D.** The culture supernatant of NS, treated as in **C**, was checked spectrophotometrically for the extracellular activity of LDH after 24 h. Pooled data of patients 1-3 are presented as means ± SD (n= 3). Vs untreated cells (ctrl): * $p < 0.005$; vs cells treated with 1 µM doxorubicin (doxo): * $p < 0.02$. **E.** The activity of caspase 3 was measured fluorimetrically in NS lysates after 24 h of treatment as in **C**, in duplicates. Pooled data of patients 1-3 are presented as means ± SD (n= 3). Vs untreated cells (ctrl): * $p < 0.02$; vs cells treated with 1 µM doxorubicin (doxo): * $p < 0.02$. **F.** Cell viability of NS, , treated as in **C**, was measured after 48 h by a chemiluminescence-based assay, in quadruplicates. Pooled data of patients 1-3 are presented as means ± SD (n= 3). Vs untreated cells (ctrl): * $p < 0.05$; vs cells treated with 1 µM doxorubicin (doxo): * $p < 0.05$.